expression of the urea cycle-related genes, including *Otc* and *Ornt 1*, dramatically decreased (Supplementary Fig. S1b). As previously discussed, cell polarity affects the distribution of intracellular organelles, including mitochondria (Braiterman and Hubbard 2010), as well as the localization of transporter molecules. Changes in the position of these components likely play a role in the often large experimental gap between assays using primary hepatocyte cultures and animals. We demonstrated this concept by showing that the results we obtained with NH_4^+, addition of L-ornithine to cultures could not suppress the release of ALT, AST, and LDH (Supplementary Fig. S2a), nor maintain cell viability (Supplementary Fig. S1b) of primary hepatocytes monolayer cultured in the presence of 3 % ethanol. Urea and NH_4^+ production by primary hepatocytes was not changed by the addition of L-ornithine in the presence of 3 % ethanol (Supplementary Fig. S1c, d), suggesting that L-ornithine has no effect on primary hepatocytes cultured under these conditions. With regard to these concerns, the liver tissue model includes several improvements that better mimic the in vivo situation. Our system of IVL^{mES} exhibits higher expression of liver-specific genes, improved ammonia degradation (Ogawa et al. 2005), and greater cytochrome P450 activity (Tsutsui et al. 2006) as compared to primary hepatocyte cultures. MRP2 is an efflux transporter expressed on the apical membrane of polarized cells (Harris et al. 2001). We previously showed that the expression of the MRP2 gene was also confirmed in IVL^{mES} by RT-PCR (Tamai et al. 2011). Based on these findings, the IVL^{mES} is expected to be able to mimic in vivo liver function. In support of this proposal, the results of the IVL^{mES} experiment assessing the hepatoprotective abilities of L-ornithine (Fig. 3) were corresponding to those in (Vogels et al. 1997) report in that blood ammonia concentration in L-ornithine-treated rats decreased gradually. These results suggest that L-ornithine in the IVL^{mES} culture medium was incorporated into hepatocyte mitochondria by ORNT1, and then converted to citrulline. The IVL^{mES} represents the possibility for high-throughput drug screening, especially as compared to the liver perfusion system, which is highly labor intensive and expensive. Hepatocytes in the IVL^{mES} are polarized in a similar fashion to their in vivo counterparts, a feature that we hypothesize is critical for their maintenance of hepatocyte functional attributes. We believe that this model system has great promise to supplant animal experiments for drug toxicity studies and experiments dissecting mechanisms of liver injury.

Acknowledgments This study was supported by a Grant-in-Aid for Scientific Research (B) (No. 21300178) from the Japan Society for the Promotion of Science (JSPS); and a Grant-in-Aid for Scientific Research on Innovative Areas (No. 23119003) from the Ministry of Education, Culture, Sports, Science and Technology (MEXT) of Japan. Miho Tamai was supported by a Research Fellowship from JSPS. The authors thank all of the members of our laboratory for their excellent assistance providing animal care.

Conflict of interest The authors declare that they have no conflict of interest.

References

Braiterman LT, Hubbard AL (2010) Hepatocyte surface polarity: its dynamic maintenance and establishment. In: Arias I (ed) The liver: biology and pathobiology, 5th edn. Wiley-Blackwell, New york, pp 73–106

Cutinelli L, Sorrentino L, Tramonti C, Salvatore F, Cedrangolo F (1970) Protection by ornithine-aspartate of the effects of physical exercise. Alzneimittel-Forschung 20:1064–1067

Demura S, Yamada T, Yamaji S, Komatsu M, Morishita K (2010) The effect of L-ornithine hydrochloride ingestion on performance during incremental exhaustive ergometer bicycle exercise and ammonia metabolism during and after exercise. Eur J Clin Nutr 64:1166–1171

Guguen-Guillouzo C, Guillouzo A (2010) General review on in vitro hepatocyte models and their applications. Meth Mol Biol 640:1–40

Harris MJ, Kuwano M, Webb M, Board PG (2001) Identification of the apical membrane-targeting signal of the multidrug resistance-associated protein 2 (MRP2/MOAT). J Biol Chem 276:20876–20881

Indiveri C, Tonazzi A, Palmieri F (1992) Identification and purification of the ornithine/citrulline carrier from rat liver mitochondria. Eur J Biochem 207:449–454

Kong X, Tan B, Yin Y, Gao H, Li X, Jaeger LA, Bazer FW, Wu G (2012) L-Arginine stimulates the mTOR signaling pathway and protein synthesis in porcine trophectoderm cells. J Nutr Biochem 23:1178–1183

Krebs HA, Henseleit K (1932) Untersuchengen über die Harntoffbildung im Tierkörper. Hoppe-Seyler's Z. fur Physiol Chem 210:33–66

Lehninger AL, Nelson DL, Cox MM (1993) Principles of biochemistry, 2nd edn. Worth, New York, p 1013

Ogawa S, Tagawa Y, Kamiyoshi A, Suzuki A, Nakayama J, Hashikura Y, Miyagawa S (2005) Crucial roles of mesodermal cell lineages in a murine embryonic stem cell-derived in vitro liver organogenesis system. Stem Cells 23:903–913

Rodriguez-Antona C, Jover R, Gomez-Lechon MJ, Castell JV (2000) Quantitative RT-PCR measurement of human cytochrome P-450 s: application to drug induction studies. Arch Biochem Biophys 376:109–116

Seglen PO (1976) Preparation of isolated rat liver cells. Meth Cell Biol 13:29–83

Tamai M, Yamashita A, Tagawa Y (2011) Mitochondrial development of the in vitro hepatic organogenesis model with simultaneous cardiac mesoderm differentiation from murine induced pluripotent stem cells. J Biosci Bioeng 112:495–500

Tirona RG, Lee W, Leake BF, Lan LB, Cline CB, Lamba V, Parviz F, Duncan SA, Inoue Y, Gonzalez FJ, Schuetz EG, Kim RB (2003) The orphan nuclear receptor HNF4alpha determines PXR- and CAR-mediated xenobiotic induction of CYP3A4. Nat Med 9:220–224

Toyoda Y, Tamai M, Kashikura K, Kobayashi S, Fujiyama Y, Soga T, Tagawa Y (2012) Acetaminophen-induced hepatotoxicity in a liver tissue model consisting of primary hepatocytes assembling around an endothelial cell network. Drug Metab Dispos 40:169–177

Tsutsui M, Ogawa S, Inada Y, Tomioka E, Kamiyoshi A, Tanaka S, Kishida T, Nishiyama M, Murakami M, Kuroda J, Hashikura Y, Miyagawa S, Satoh F, Shibata N, Tagawa Y (2006) Characterization of cytochrome P450 expression in murine embryonic stem cell-derived hepatic tissue system. Drug Metabol Dispos Biol Fate Chem 34:696–701

Underhill GH, Khetani SR, Chen AA, Bhatia SN (2010) Tissue engineering of the liver. In: Arias IM (ed) The liver: biology and pathobiology, 5th edn. Wiley-Blackwell, New York, pp 935–954

Vogels BA, Karlsen OT, Mass MA, Bovee WM, Chamuleau RA (1997) L-ornithine versus L-ornithine-L-aspartate as a treatment for hyperammonemia-induced encephalopathy in rats. J Hepatol 26:174–182

Zeng L, Tan B, Yin Y, Kong X, Fen Z, Fang J, Lu X (2012) Gene expression profiles in porcine intestinal epithelial cells treated with arginine using a microarray technique. J Food Agri Environ 10:834–839

Journal of Bioscience and Bioengineering
VOL. 117 No. 1, 99–106, 2014

ELSEVIER

www.elsevier.com/locate/jbiosc

Hybrid sponge comprised of galactosylated chitosan and hyaluronic acid mediates the co-culture of hepatocytes and endothelial cells

Yi Shang,[1] Miho Tamai,[1] Ryusei Ishii,[1] Noriyuki Nagaoka,[2] Yasuhiro Yoshida,[2] Masamichi Ogasawara,[3] Jun Yang,[4] and Yoh-ichi Tagawa[1,*]

Department of Biomolecular Engineering, Graduate School of Bioscience and Biotechnology, Tokyo Institute of Technology, 4259 B51, Nagatsuta-cho, Midori-ku, Yokohama, Kanagawa 226-8503, Japan,[1] Okayama University Graduate School of Medicine, Dentistry and Pharmaceutical Sciences, 2-5-1 Shikata-cho, Kita-ku, Okayama 700-8525, Japan,[2] Catalysis Research Center and Graduate School of Life Science, Hokkaido University, Kita-ku, Sapporo 001-0021, Japan,[3] and The Key Laboratory of Bioactive Materials, Ministry of Education, College of Life Science, Nankai University, No. 94 Weijin Road, Tianjin 300071, PR China[4]

Received 10 June 2013; accepted 14 June 2013
Available online 27 July 2013

When constructing an *in vitro* model of liver tissue to mimic the *in vivo* liver microenvironment, the major challenge is to preserve and maintain the hepatocyte phenotype. The aim of this study was to develop a novel intelligent hybrid sponge for use in a dense co-culture system designed to simulate the liver microenvironment. We prepared a galactosylated chitosan (GCs)/hyaluronic acid (HA) hybrid sponge using a freeze-drying technique for the co-culture of primary hepatocytes and endothelial cells. Subsequently, we investigated the biocompatibility of the GCs/HA scaffold with primary hepatocytes and endothelial cells in terms of cell attachment, morphology, bioactivity, and maintenance of specific liver functions. The GCs/HA-hybrid sponge demonstrated good biocompatibility not only with primary hepatocytes, but also with endothelial cells. In our model, primary hepatocytes exhibited superior bioactivity and higher levels of liver-specific functions in terms of hepatocyte-specific gene expression, urea production, and testosterone metabolism as compared to a monoculture system. We succeeded in constructing a liver tissue-like model using the GCs/HA-hybrid sponge. Therefore, we anticipate that GCs/HA-hybrid sponges may be a promising matrix for the co-culture of hepatocytes and endothelial cells in liver tissue engineering, and might be employed as a novel co-culture model for applications in toxicology and drug metabolism.

[**Key words:** Liver; Tissue; Galactosylated chitosan; Hyaluronic acid; Primary hepatocyte; Endothelial cell]

The liver is an organ of considerable cellular heterogeneity with hepatic lobules consisting of parenchymal hepatocytes, non-parenchymal cells (e.g., sinusoidal endothelial, stellate, and Kupffer cells), and some extracellular matrices (ECMs) comprising proteins, glycosaminoglycans, glycoproteins, and proteoglycans. Hepatocytes observed *in situ* within the liver exhibit a polygonal morphology; however, hepatocytes grown *in vitro* as monolayers are flat. Hepatocytes are thought to be able to fully execute liver-specific functions only in the context of the proper structural microenvironment represented by intact liver tissue. Because primary hepatocytes cultured as monolayers quickly lose structural polarity, it is difficult to use those cultures for assays of hepatic functions, e.g., drug metabolism. Therefore, it remains a major challenge for tissue engineers to develop intelligent scaffold materials that can recapitulate the liver microenvironment in an *in vitro* model system. In this context, we focused on a very dense co-culture system of hepatocytes and endothelial cells that closely resembles the major cell populations found in the intact liver.

In 2005, we successfully achieved hepatic organogenesis from murine ES/iPS cells (1–3). This mouse ES cell–derived *in vitro* liver tissue model, IVL^{mES}, included both hepatocyte layers and a vascular-like endothelial cell network; the model was capable of recapitulating most hepatic functions. Furthermore, another *in vitro* liver model, $IVL^{PH\&HUVEC}$, using primary hepatocytes, human umbilical vein endothelial cells (HUVECs), and Engelbreth–Holm–Swarm (EHS) gel was also established for use in a drug metabolism assay (4). While the EHS gel contains a variety of extracellular matrix components secreted from the EHS tumor, an ideal *in vitro* liver model would use constituent-defined materials that would provide a uniform background for the development of pharmacokinetics assays and artificial liver systems. Hyaluronic acid (HA), a ligand for endothelial cell-expressed CD44, was expected to be useful for the co-culture of hepatocytes and endothelial cells (5–7). In this study, we designed a new galactosylated chitosan (GCs)/HA scaffold that was expected to bind to both hepatocytes (through GCs) and endothelial cells (through HA), as can be seen in Fig. 1, and succeeded to construct a liver tissue-like model consisting of hepatocytes and endothelial cells on a GCs/HA sponge.

MATERIALS AND METHODS

Materials Chitosan (Cs) (viscosity: 25~75 cps; molecular weight: 6×10^5; degree of deacetylation: 80%), 1-ethyl-(dimethylaminopropyl) carbodiimide (EDC), *N′,N′,N′*-tetramethylethylethylene diamine (TEMED), and Sulfo-*N*-

* Corresponding author. Tel.: +81 45 924 5791; fax: +81 45 924 5809.
E-mail address: ytagawa@bio.titech.ac.jp (Y. Tagawa).

1389-1723/$ – see front matter
http://dx.doi.org/10.1016/j.jbiosc.2013.06.015

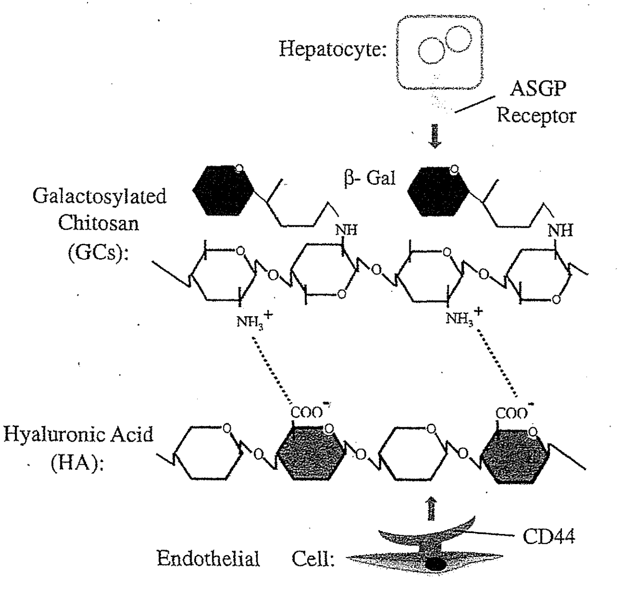

FIG. 1. The GCs/HA sponge is designed to bind both hepatocytes and endothelial cells by engaging specific cell-surface receptors on each cell type.

hydroxylsuccinimide (NHS) were purchased from Wako Pure Chemical Industries, Ltd. (Osaka, Japan). HA with viscous average molecular weight 8×10^5 was kindly gifted from Dr. Mitsuaki Goto, Molecular Engineering Institute, Kinki University (Fukuoka, Japan). Lactobionic acid (LA) was purchased from Sigma Chemical Co. (St. Louis, MO, USA).

Synthesis of GCs GCs was prepared from the reaction of Cs with LA by the method previously reported (8). Briefly, 12 mmol of LA was dissolved in 50 mL of 10 mM TEMED/HCl buffer (pH 4.7) and activated with a mixture of Sulfo-NHS (1.2 mmol) and EDC (12 mmol), and then reacted with Cs (24 mmol). The reaction was performed for 72 h at room temperature. The obtained GCs was purified by dialysis against Milli Q water for one week and then lyophilized.

Preparation of GCs/HA, GCs, and Cs sponges GCs/HA sponge was fabricated as follows: 2% GCs was dissolved in 0.5 M acetic acid aqueous solution by continuously stirring to form a homogenous solution, and mixed with 1% HA aqueous solution with a volume ratio of 1:1, followed by homogenizing for 20 min. Then, 0.2 mL of the obtained solution was poured into each well of 48-well polystyrene culture plates. The plates were frozen at −20°C, followed by freeze-drying to form a porous structure.

GCs and Cs sponges were prepared as described above. Briefly, 0.2 mL of 1% GCs and Cs solution was poured into each well of 48-well polystyrene culture plates and freeze-dried. Lyophilized sponges were treated by a gradient ethanol process. Before cell culture, the sponges were sterilized by ethylene oxide gas.

Scanning electron microscopy (SEM) The morphology of GCs/HA, GCs, and Cs sponges was observed by SEM (Topcon DS-720, Tokyo, Japan). The sponges were cut with a sharp scalpel, and then mounted onto an aluminum stub and sputter-coated with gold–palladium. Mean pore diameters were estimated by analysis of digital SEM images. Average pore sizes were determined based on the sizes of 40 pores for each sample.

Fourier transform infrared spectroscopy (FTIR) and ^{1}H nuclear magnetic resonance (^{1}H NMR) FTIR spectra were measured using a Nicolet 5700 FTIR spectrometer (Thermo Electron Co., WI, USA). Dried samples were ground with KBr powder and compressed into pellets for FTIR examination.

^{1}H NMR (600 MHz) spectra were recorded on an ECX-600 spectrometer (JEOL, Tokyo, Japan). The samples were dissolved in a 2/98 mixture of CD_3COOD/D_2O at a concentration of ca. 5 mg/mL.

Animals Male, 6–8 week old, DsRed2 C57BL/6 transgenic mice that constitutively and ubiquitously express the DsRed2 gene under the control of the CAG promoter (9) were used in this study. The experiments were conducted according to institutional ethical guidelines for animal experiments and safety guidelines for recombinant DNA experiments.

Isolation and culture of murine primary hepatocytes Red fluorescent hepatocytes were harvested from DsRed2 transgenic mice using a two-step *in situ* collagenase perfusion procedure (10) with slight modifications (4). Briefly, the liver was perfused with perfusion buffer and collagenase buffer by cannulation of the isolated portal vein with a 24-gauge catheter (Terumo, Tokyo, Japan). Then, the perfused liver was dissected, suspended in Hank's Buffered Salt Solution (HBSS), and filtered through a 100 μm pore mesh nylon cell strainer (BD Biosciences, Bedford, MA, USA). Hepatocytes were purified by density-gradient centrifugation (50 ×g, 10 min) using a 36% Percoll solution (GE Healthcare, Tokyo, Japan) at 4°C. Cell viability as measured by trypan blue exclusion was >90%. The primary hepatocytes were cultured with 10% FBS/William's medium E containing antibiotics (100 U/mL penicillin and 100 μg/mL streptomycin).

Endothelial cells EAhy926 cells, generously provided by Dr. Cora-Jean S. Edgell, of the University of North Carolina, USA, were established by fusing primary human umbilical vein endothelial cells (HUVECs) with human lung adenocarcinoma epithelial cells (A549) (11). An enhanced green fluorescent protein (EGFP) gene-expressing EAhy926 cell line, GH7, was established by the introduction of the appropriate expression vector under control of the CAG promoter. The cells were cultured in DMEM (Invitrogen, Tokyo, Japan) supplemented with 10% FBS and antibiotics (100 U/mL penicillin and 100 μg/mL streptomycin) in a humidified atmosphere of 5% CO_2/95% air at 37°C. The medium was replaced every other day. When confluent, the cells were detached by trypsinization (0.05% trypsin and 0.53 mM EDTA), resuspended in medium, and split for subculture. To block proliferation, GH7 cells were incubated in the presence of 10 μg/ml mitomycin C for 3 h before seeding on culture scaffolds.

Culture of primary hepatocytes and GH7 cells in sponges To culture primary hepatocytes and/or GH7 cells on three-dimensional Cs, GCs and GCs/HA-hybrid sponges, cells were seeded at $1–3 \times 10^5$ per sponge and cultured with William's E medium. The cells were observed using a fluorescence inverted microscope (Olympus, Tokyo, Japan).

Fluorescence intensity assay In order to quantitate the number of living cells, DsRed2 and EGFP fluorescence intensities were measured by using the LAS-4000 system (Fujifilm, Tokyo, Japan). Images were analyzed using the ImageJ Multi Gauge program version 3.1 (Fujifilm).

WST-8 assay Adherent cells were washed three times with PBS. Subsequently, fresh medium containing 10% (v/v) of WST-8 (Nacalai Tesque, Kyoto, Japan) was added, cells were incubated for 1 h, and 100 μL of the resulting supernatant was transferred to a 96-well microplate. The reduction of WST-8 was measured photometrically using an iMark Microplate Reader (Bio-Rad Laboratories, Hercules, CA, USA) at 450 nm.

Histological and immunofluorescence assessment The cell-incorporating sponges were fixed in 4% paraformaldehyde, embedded in paraffin, sectioned (5 μm), and stained with hematoxylin and eosin (H&E) for histological evaluation. For immunofluorescence staining, sections were heated at 60°C for 1 min, deparaffinized in xylene, and rehydrated through graded ethanol to Milli Q water. The sections were washed three times with PBS and then incubated in Blocking One buffer (Nacalai Tesque) for 30 min at room temperature. Then, the slides were incubated with primary antibodies, including rabbit anti-red fluorescent protein IgG (1:500; Medical and Biological Laboratories, Nagoya, Japan) and goat anti-green fluorescent protein IgG (1:1000; Abcam, Tokyo, Japan) for 2 h at room temperature. Next, sections were incubated with 4′,6-diamidino-2-phenylindole (DAPI), donkey anti-rabbit IgG conjugated with Alexa Fluor 594 (1:2000; Invitrogen) and donkey anti-goat IgG conjugated with Alexa Fluor 488 (1:2000; Invitrogen) for 1 h at room temperature. Finally, the sections were mounted in Prolong Gold fluorescent mounting medium (Invitrogen).

Total RNA preparation and reverse transcriptase-polymerase chain reaction (RT-PCR) Total RNA was isolated from cells in the sponges using the cetyltrimethylammonium bromide (CTAB) method (12) because it was difficult to prepare RNA using the general method due to the contamination of polysaccharide scaffold materials. The purity and concentration of isolated RNA was assessed by UV absorbance, and RNA integrity was verified by 0.6% agarose gel electrophoresis in TAE buffer. First strand cDNA was prepared from the extracted total RNA in a reverse transcriptase reaction, using the SuperScript II Reverse Transcriptase kit and oligo dT primers (Invitrogen) according to the manufacturer's instructions. The cDNA corresponding to the genes of interest (Table 1) was amplified by PCR in a GeneAmp PCR System 9700 thermal cycler (Applied Biosystems, Tokyo, Japan). After initial denaturation at 94°C for 1 min, PCR amplification was continued at 94°C for 30 s, at the annealing temperature for 30 s, and at 72°C for 30 s for a total 30–40 cycles, with a final extension at 72°C for 10 min. Amplified DNA fragments were separated by 1.5% (w/v) agarose gel electrophoresis with TBE buffer. The gels were stained with ethidium bromide (10 μg/mL) and photographed on a UV transilluminator (Bio-Rad Laboratories). For quantitative analysis of albumin *(Alb)* expression, real-time PCR was carried out by using the StepOnePlus Sequence Detection System (Applied Biosystems). Hypoxanthine-guanine phosphoribosyltransferase (*Hprt*) was used as an internal housekeeping reference. Gene expression was quantified using the ΔΔCt method.

Urea assay During the culture period, conditioned medium (CM) samples were collected every day and stored at −20°C until assayed using a QuantiChrom Urea Assay Kit (BioAssay Systems, Hayward, CA, USA). Briefly, 50 μL of CM were incubated with 200 μL of the reaction mixture for 20 min at room temperature. The urea-dependent chromogenic reaction was read using an iMark Microplate Reader (Bio-Rad Laboratories) at 490 nm. The urea concentration was determined using a standard curve.

Testosterone metabolism assay To examine the enzymatic activities of cytochrome P450s, each metabolite of testosterone in the culture medium was quantitatively detected using high performance liquid chromatography (HPLC) as

TABLE 1. Primer information for mouse gene.

Gene	GenBank ID	F/R	Sequences (5'->3')	Position	Product (bp)
Alb	NM_009654	F	GCTACGGCACAGTGCTTG	1224–1241	266
		R	CAGGATTGCAGACAGATAGTC	1489–1469	
Tat	NM_146214	F	CAATCCTGGACAGAACATCC	565–584	280
		R	GATCTCATCGGCTAAGATGG	844–825	
Cyp2e1	NM_021282	F	TGTGACTTTGGCCGACCTGTTC	889–910	446
		R	CAACACACACGCGCTTTCCTGC	1334–1313	
Cps1	NM_001080809.1	F	TGCCAATGTGACTACGAAGC	159–178	425
		R	AAATTGCAGGGACCTTTTCC	583–564	
Arg1	NM_007482.3	F	TCACCTGAGCTTTGATGTCG	783–802	252
		R	TTACCCTCCCGTTGAGTTCC	1034–1015	
Otc	NM_008769.3	F	GAAAGGGTCACACTTCTGTGG	122–142	264
		R	GAGCAAAGCCTGTTTCTGTGG	385–365	
Ornt1	NM_181325.4	F	GTGGTCCGTAAAGTGGTTGG	513–532	252
		R	TGAGAGCCCATGGTAGAAGC	764–745	
Hprt	NM_013556	F	GTAATGATCAGTCAACGGGG	463–482	441
		R	AGCTTTACTAGGCAGATGGC	903–884	
Hprt[a]	NM_013556.2	F	GTCAACGGGGGACATAAAAG	473–492	128
		R	GCTTAACCAGGGAAAGCAAAG	600–580	
Alb[a]	NM_009654.3	F	AAAACCCAACCACCACCTATGG	504–524	218
		R	GGAGCACTTCATTCTCTGACG	721–701	

[a] Real-time PCR; F, forward; R, reverse.

described previously (3). Briefly, the cells incubated for 24 h at 37°C with the culture medium containing 0.25 mM testosterone (Sigma). After incubation, the reaction was terminated by aspirating the medium from the plates. The amounts of testosterone metabolite products, 6β and 7α-OH testosterones were measured using an HPLC system (LC-10AD VP, Shimadzu, Kyoto, Japan). equipped with a reversed-phase C18 column (Cadenza CD-C18, 10 mm × 250 mm; Tosoh, Tokyo, Japan) maintained at 40°C. Elution solvents were: solvent A (water/methanol/acetonitrile: 39:60:1 v/v) and solvent B (water/methanol/acetonitrile: 80:18:2 v/v). Elution was started with 18% solvent B and 82% solvent A for 10 min, followed by elution with a linear gradient of solvent B (18–80%) for the next 10 min. Afterward, 80% solvent B was maintained for 30 min. The elution flow throughout was kept constant at a rate of 0.5 mL/min, and testosterones were detected by UV absorbance at 254 nm. The resulting chromatograms were analyzed using the LC Solutions software (Shimadzu). The peak of each metabolite was compared with that of the internal standard in order to determine its quantity. To obtain the standard chromatogram, 6β and 7α-OH testosterones were subjected to independent analyses.

Statistical analysis Results were presented as means ± S.E., and statistically analyzed by the Student's *t*-test. Values of $p < 0.05$ were considered statistically significant.

RESULTS

Adhesion of primary hepatocytes/endothelial cells to scaffolds of GCs/HA GCs, prepared from the reaction of Cs with LA, was confirmed by FTIR. The characteristic absorption peaks 1646 and 1594 cm^{-1}, which were contributed to I and II amides were observed in Cs, on the other hand, these peaks were slightly shifted to 1616 and 1554 cm^{-1}, respectively in GCs (Fig. S1), indicating that the amide bond was formed between the carboxylic of LA and amine groups of chitosan with activation agents of EDC and NHS, that is, LA was introduced into Cs chains. The ^1H NMR spectra of GCs and Cs were measured to calculate the efficiency of the grafting of LA in GCs. The efficiency of the grafting of LA in GCs was estimated by 15 mol% from the characteristic peak areas of LA group (4.1 ppm) with that of ~2.0 ppm peak attributed to the original acetamide group of Cs in ^1H NMR spectra of GCs and Cs (Fig. S2).

To confirm the adhesion of hepatocytes to the galactose residue on the Cs-backbone scaffold as shown in Fig. 1, red fluorescent primary hepatocytes, prepared from the liver of a DsRed2 transgenic mouse, were seeded at 5×10^4 cells/well on Cs- or GCs-coated 24-well polystyrene plates for 4 h. As shown in Fig. 2A, hepatocytes could non-specific adhere on Cs, however, the hepatocytes were much more adherent to GCs as compared to Cs. In order to quantify the cell adhesion by fluorescence intensity, we investigated the relationship between practical adhered cell numbers and the corresponding fluorescence intensity. As shown in Fig. 2B, the practical number of the adhered hepatocytes was proportional to the fluorescence intensity. The amount of cell adhesion on Cs- or GCs-coated plate, calculated from the fluorescence images, was significantly higher on the GCs-coated plates than on the Cs-coated plates (Fig. 2C). The WST-8 assay also supported the interpretation that the hepatocytes preferentially adhered to GCs (Fig. 2D). These results suggest that the presence of a galactose residue enhanced hepatocyte attachment to the Cs-backbone scaffold.

Next, to investigate the interaction between endothelial cells and HA, green fluorescence endothelial cells (GH7) were seeded at 5×10^4 cells/well on 24-well polystyrene plates coated for 4 h with solutions containing increasing concentrations of HA (e.g., 0%, 0.05%, 0.1%, and 0.5%). GH7 cells tended to adhere to HA in a concentration dependent fashion (Fig. 3A), and, on this substrate, the cells exhibited a spread morphology; however, they could slightly adhere and maintained a rounded shape on a non-HA-coated plate. As we observed a linear relationship between EGFP fluorescence signal intensities and the practical number of adhered GH7 cells (Fig. 3B), the number of adherent cells was calculated by fluorescence (Fig. 3C). Adhesion of GH7 cells increased with the percentage of HA in the coating solution, yielding the same results observed in the WST-8 experiments (Fig. 3D). Together, these data suggested that GH7 recognizes and binds to the scaffold HA.

Preparation and structural features of GCs/HA, GCs, and Cs sponges We expected that electrostatic effects would induce interactions between the amines on GCs and the carboxyl groups on HA (Fig. 1). Therefore, 2% GCs in an acetic acid solution was mixed with 1% HA in an aqueous solution at a 1:1 ratio (v/v), and was homogenized for 20 min. Next, the solution was aliquoted (0.2 mL/well) into a 48-well polystyrene culture plate and frozen at −20°C. Then, the plates were lyophilized, yielding a sponge-like porous structure in the wells. GCs and Cs sponges, as controls, were also prepared in the same manner. The sponge diameter and thickness was 8.7 ± 0.3 mm and 1.9 ± 0.2 mm, respectively. SEM analysis revealed open pore microstructures with a high degree of interconnectivity in the each sponge (Fig. 4A). The pore size within each sponge was nearly uniform. The pores in the GCs/HA sponge, at 147.5 ± 32.2 μm, were larger than those in the Cs and GCs sponges, at 126.5 ± 28.4 and 114.1 ± 22.7 μm, respectively. Furthermore, the pores in the GCs/HA sponge were more interconnected than were those in the sponges made from GCs or Cs alone.

The GCs/HA-hybrid sponge was biocompatible with primary hepatocytes and endothelial cells Freshly isolated DsRed2

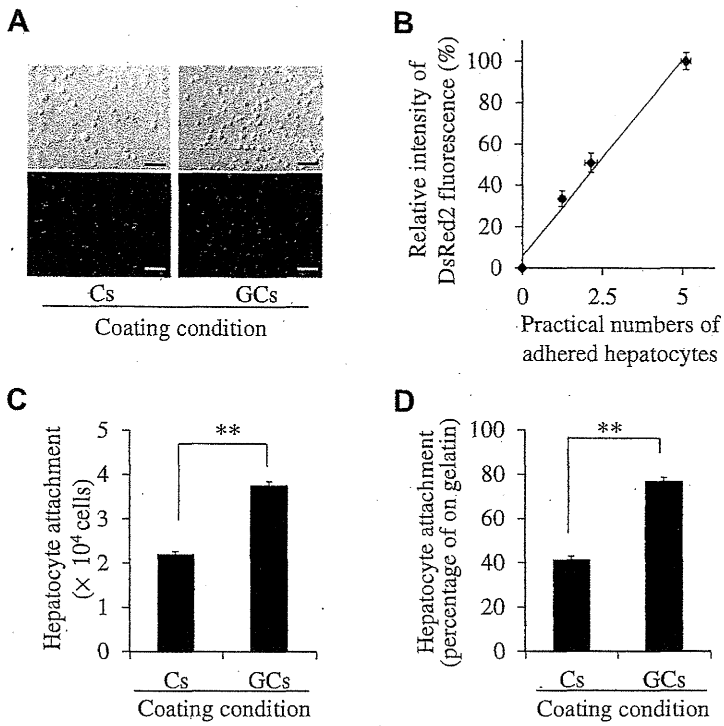

FIG. 2. Adhesion of primary hepatocytes to scaffolds of Cs or GCs. (A) Adhesion of primary DsRed2 hepatocytes to Cs-, or GCs-coated plates after 4 h in culture as seen using the optical (top) and fluorescence filters (bottom). Scale bars: 100 μm. (B) The linear relationship between the signal intensity of DsRed2 fluorescence and the total amount of practical adhered hepatocytes on gelatin after 4 h in culture. When the practical adhered red hepatocytes numbers is 5×10^4 cells per well in 24-well plate on gelatin, the fluorescence intensity was defined as 100%. (C) The hepatocyte attachment level on GCs- or Cs-coated derived from the intensity of DsRed2 fluorescence. Fluorescent images were obtained 4 h after the seeding of primary hepatocytes and were analyzed by the ImageJ Multi Gauge program. (D) Quantification of primary hepatocyte adhesion on Cs- or GCs-coated plates using the WST-8 assay. Data are calculated as ratios by referring to the hepatocyte adhesion on gelatin coated plate. Data are represented as mean ± S.E. of triplicate measurements. $^{**}p < 0.01$.

hepatocytes were seeded at a cell density of 4×10^5 cells/sponge on Cs, GCs, or GCs/HA sponges and cultured with serum-free William's E medium at 37°C for 24 h. Fig. 4B shows the number of hepatocytes that adhered to GCs/HA and GCs sponges, as compared to the Cs sponges. Cell adhesion in these sponges was quantified by the WST-8 assay. The amount of cell adhesion was significantly higher on the GCs and GCs/HA sponges than on the Cs sponge (Fig. 4D).

DsRed2 hepatocytes are primary cells that cannot proliferate, while GH7 is a proliferating cell line. To stop the proliferation of GH7 cells prior to the experimental period, the cells were treated with 10 μg/mL mitomycin C for 3 h. Then, mitomycin C–treated GH7 cells were seeded at 4×10^5 cells/sponge on the Cs, GCs, or GCs/HA sponges for 24 h. Fig. 4C shows that a considerable amount of GH7 cells adhered to the GCs/HA scaffold as compared to the GCs and Cs sponges. Cell adhesion levels in these sponges were quantified by the WST-8 assay. The cell adhesion level was significantly higher on the GCs/HA sponges than on the Cs and GCs varieties (Fig. 4E).

These results were consistent with those made in the scaffold materials plate-coating experiment (Figs. 2 and 3) and indicate that the GCs/HA-hybrid sponge exhibits favorable biocompatibility with both hepatocytes and endothelial cells.

Characterization of primary hepatocytes and endothelial cells cultured on a GCs/HA-hybrid sponge DsRed2 hepatocytes and GH7 cells were seeded together at a density of 3×10^5 and 1×10^5 cells, respectively, in 100 μL culture medium onto a dry GCs/HA sponge in one well of a 48-well polystyrene plate. Fresh culture medium was supplied daily for 7 days. As shown in Fig. 5A and B, both hepatocytes and GH7 cells survived and formed clusters by day 7.

Seeded sponges were 4% paraformaldehyde-fixed at days 1 and 7, and prepared for histological examination with H&E staining and immunolabeling with anti-GFP and anti-DsRed antibodies. Fig. 5C and D illustrates that cells adhered to and penetrated the GCs/HA sponges at days 1 and 7, and that most of the hepatocytes were round or spherical in shape without extending their pseudopods and form clusters. The GCs/HA sponge kept its porous structure and pore interconnections throughout the culture period, which allowed for the facile exchange of nutrients and waste products within the scaffold, supporting robust cell proliferation and differentiation. The hepatocytes and GH7 cells were uniformly distributed throughout the sponge during the culture period (Fig. 5E and F).

We used RT-PCR analysis to compare hepatocyte-specific gene expression when cells grown in the GCs/HA-hybrid sponge between a hepatocyte monoculture system vs. those grown in the hepatocyte/endothelial cell sponge co-culture system, and cells cultured on Cs sponge and GCs sponge as control culture conditions, were also evaluated.

The expression of *Alb*, tyrosine aminotransferase (*Tat*), cytochorome P450 (*Cyp*) 2e1 genes, and urea cycle related genes, such as ornithine transcarbamoylase (*Otc*), arginase 1 (*Arg1*), carbamoyl phosphate synthetase 1 (*Cps1*), and ornithine/citrulline transporter 1 (*Ornt1*), was strongly detected at day 1 in each culture systems (Fig. 6A). The expression of these genes was still detected at day 7 in the hepatocyte/endothelial cell sponge co-culture, but not in the hepatocyte monoculture systems, and was stronger in the GCs/HA-hybrid sponge than that in the Cs or GCs sponge whether the hepatocytes were cultured with or without GH7 cells. The real-time PCR examination also indicates that the expression of *Alb* was significantly higher in the co-culture system on GCs/HA-hybrid sponge than other culture conditions (Fig. 6B).

Finally, the liver-specific biochemical metabolites of hepatocytes on Cs, GCs and GCs/HA-hybrid sponges, such as those obtained during urea production were quantified in the media at days 1, 4

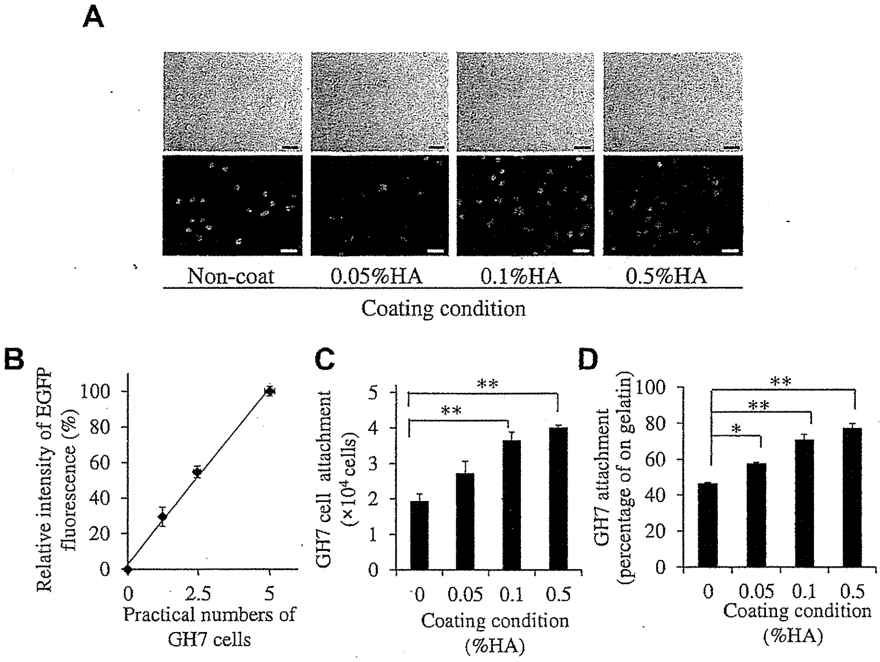

FIG. 3. Adhesion of endothelial cells to scaffolds of HA. (A) GH7 cell adhesion on plates coated with different concentrations of HA as seen using the optical (top) and fluorescence filters (bottom). Scale bars: 50 μm. (B) The linear relationship between the signal intensity of EGFP fluorescence and the total amount of practical adhered GH7 cells on gelatin after 4 h in culture. When the practical adhered GH7 cell numbers is 5×10^4 cells per well in 24-well plate on gelatin, the fluorescence intensity was defined as 100%. (C) The GH7 cell attachment level on GCs- or Cs-coated derived from the intensity of EGFP fluorescence. Fluorescent images were obtained 4 h after the seeding of GH7 cells and were analyzed by the ImageJ Multi Gauge program. (D) Quantification of GH7 cell adhesion on plates coated with different concentrations of HA using the WST-8 assay. Data are calculated as ratios by referring to the GH7 cell adhesion on gelatin coated plate. Data are represented as mean ± S.E. of triplicate measurements.$^{*}p < 0.05$; $^{**}p < 0.01$.

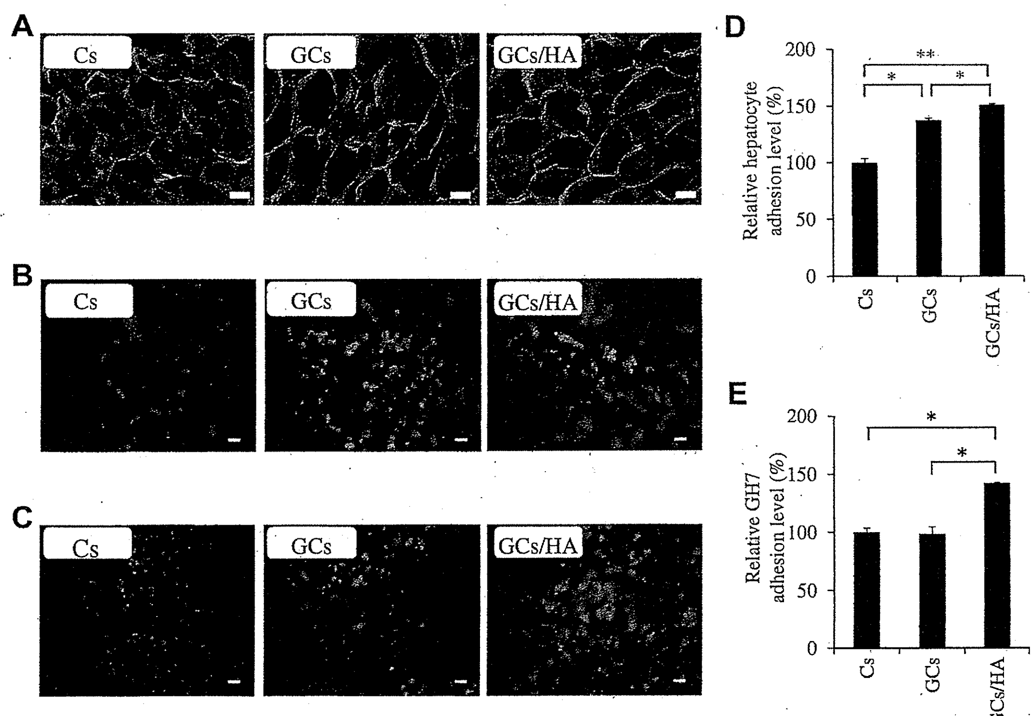

FIG. 4. Comparison of biocompatibility among Cs, GCs, and GCs/HA-hybrid sponges. (A) Scanning electron micrographs of Cs, GCs, and GCs/HA sponges. (B) Fluorescence micrographs of DsRed2 hepatocytes cultured on Cs, GCs, and GCs/HA sponges after 24 h. (C) Fluorescence micrographs of GH7 cells cultured on Cs, GCs, and GCs/HA sponges after 24 h. (D) Quantification of primary hepatocytes attached on Cs, GCs, and GCs/HA sponges using the WST-8 assay. Data are calculated as ratios by referring to the primary hepatocyte adhesion on Cs sponge. (E) Quantification of GH7 cells attached on Cs, GCs, and GCs/HA sponges using the WST-8 assay. Data are calculated as ratios by referring to the GH7 cell adhesion on Cs sponge. Data are represented as mean ± S.E. of triplicate experiments. $^{*}p < 0.05$; $^{**}p < 0.01$. Scale bars: 50 μm.

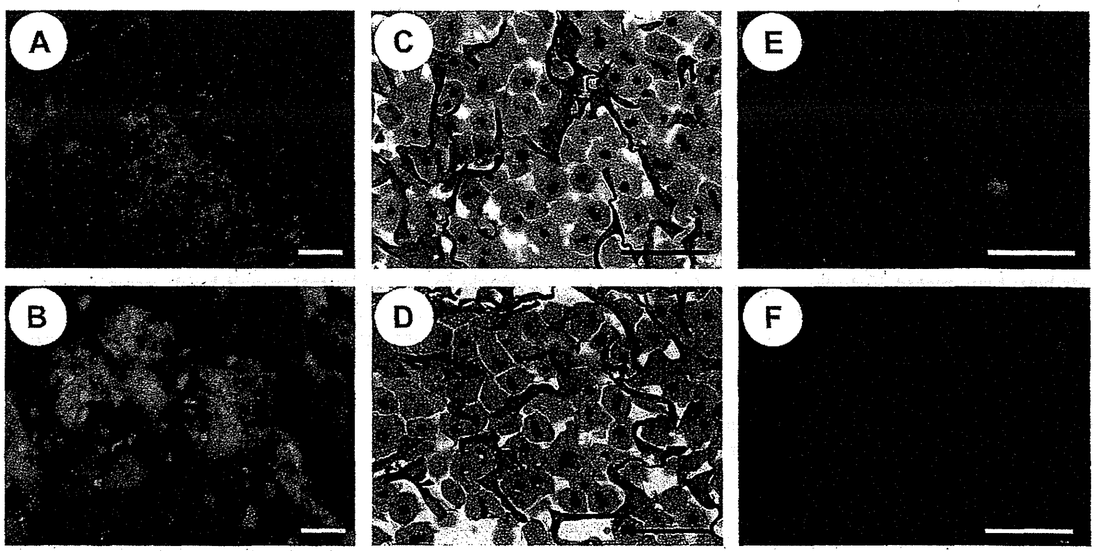

FIG. 5. Characterization of primary hepatocytes and endothelial cells cultured on a GCs/HA sponge. Fluorescence micrograph of hepatocytes and GH7 cells cultured on a GCs/HA sponge at days 1 (A) and 7 (B). HE staining of hepatocytes and GH7 cells cultured on a GCs/HA sponge at days 1 (C) and 7 (D). GFP/RFP immunofluorescence staining of hepatocytes and GH7 cells cultured on a GCs/HA sponge at days 1 (E) and 7 (F). Scale bars: 50 μm.

and 7. The results indicated that urea synthesis rapidly decreased over the culture period in the Cs or GCs sponge culture condition whether the hepatocytes were cultured with or without GH7 cells, whereas it decreased slowly and maintained higher total levels in the GCs/HA-hybrid sponge co-culture system (Fig. 6C). In addition, testosterone metabolism was investigated to quantify testosterone metabolites which received oxidation by cytochrome P450 isozymes by using HPLC in GCs/HA-hybrid sponge culture condition. The amount of 6β, 7α-OH testosterones (Cyp3a, Cyp2a4/5 and 2d9) was significantly higher in the co-culture system at day 4 (65.56 ± 5.45 nM) than that in the hepatocyte monoculture system (44.56 ± 6.61 nM).

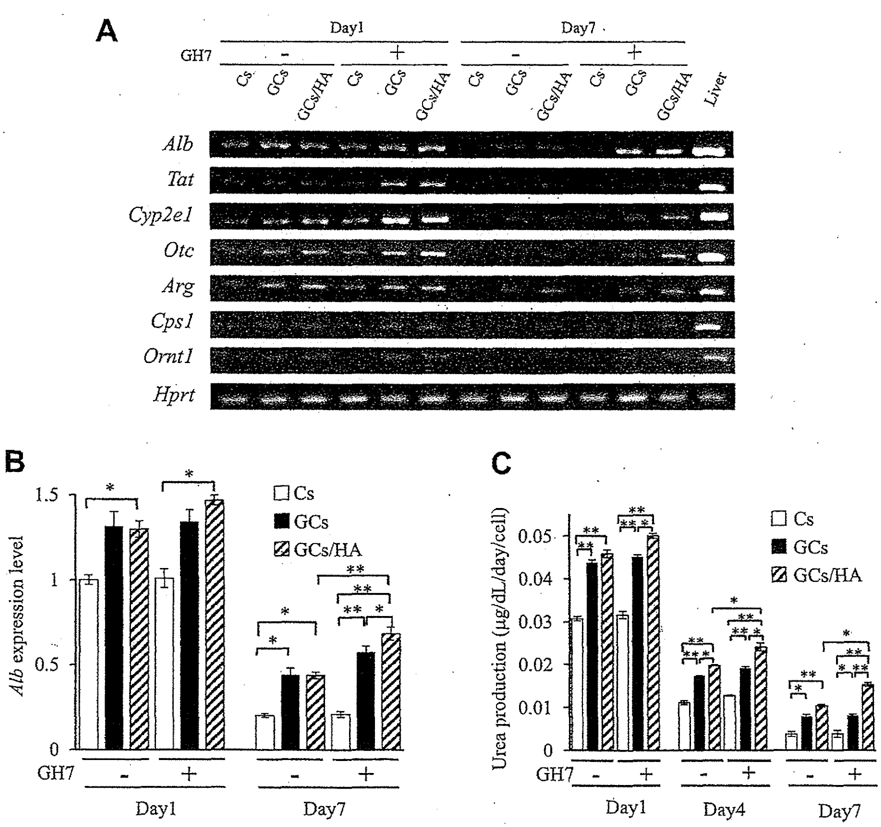

FIG. 6. Liver-specific functions of hepatocytes cultured in Cs, GCs, and GCs/HA sponges. (A) Comparison of hepatocyte-specific gene expression in different culture conditions. (B) Real-time PCR analysis of *Alb* expression in different culture conditions (open bars, Cs sponge; closed bars, GCs sponge; hatched bars, GCs/HA sponge). (C) Urea levels observed in conditioned medium from the different culture conditions (open bars, Cs sponge; closed bars, GCs sponge; hatched bars, GCs/HA sponge). Data are represented as mean ± S.E. of triplicate experiments. *$p < 0.05$; **$p < 0.01$.

DISCUSSION

Hepatocytes are anchorage-dependent cells and highly sensitive to the topography and biochemical properties of the ECM. Hepatocytes require interactions with the ECM for survival and differentiated function. Tissue engineers have found that it is necessary to suppress detachment-induced cell death (anoikis) by encouraging interactions between hepatocytes and ECM (13). To avoid loss of hepatic function and the induction of anoikis, various hepatocyte culture methods have been tested, including the use of natural, e.g., collagen, fibronectin, laminin, and synthetic ECM substrates, e.g., galactosylated materials (14,15) and E-cadherin-Fc fusion protein (16). Other materials and culture systems were developed specifically to mimic cell—cell interactions, which are also important for the maintenance of hepatic functions. For example, hollow nanofibers (15—17), hydrogel microspheres (18,19), and macroporous polymer sponges (20,21), have all been used to generate spheroid aggregate hepatocyte cultures. In this study, we used GCs as a matrix for the culture of primary hepatocytes. The galactose residue mediates robust attachment, as shown in Fig. 2A. We recently demonstrated that it was possible to culture primary hepatocytes exhibiting high hepatic functions for at least two weeks on the highly porous hybrid Cs and galactosylated hyaluronic acid sponge (20). Although HA is a ligand of endothelial cells, endothelial cells had not previously been cultured using this model system. Here, after developing the GCs/HA-hybrid sponge, we succeeded in establishing a dense co-culture system of hepatocytes and endothelial cells—thus closely mimicking the dominant cell populations in the intact liver.

We investigated specific interactions and biocompatibility between cells and materials. Compared to the GCs and Cs sponges, the GCs/HA-hybrid sponge exhibited favorable biocompatibility as demonstrated by the enhanced cell-specific functions observed during the culture period. These observations were consistent with the hypothesis that hepatocyte adhesion to GCs was mediated through galactose-specific recognition of GCs by asialoglycoprotein receptor (ASGPR) on hepatocytes. Similarly, the results supported the theory that HA could enhance endothelial cell adhesion and proliferation through interactions with its receptor CD44. ASGPR is a receptor localized on the membrane of hepatocytes facing the sinusoids, with specificity for glycoproteins with galactose. The binding of the galactose ligand to ASGPR induces liver-targeted transfer of glycoproteins (22,23). As for the interaction between endothelial cells and HA, HA provides anchorage sites for endothelial cells through the cell-surface receptor, CD44. As a result, the endothelial cells produce growth factors that promote hepatocyte adhesion and survival.

In this study, we prepared a highly porous sponge with a pore size of ~150 μm using a freeze-drying method (Fig. 4A). Previous studies have shown that a pore size larger than 100 μm provides optimum cell viability and function, with no mass transfer limitations. Our constructed scaffolds provided both mechanical and environmental support for promoting cell adhesion, penetration, cell-matrix, and cell—cell interactions, as shown in Fig. 3.

Heterotypic cell—cell interactions between hepatic parenchymal cells and non-parenchymal neighbors has been reported to play an especially important role in the preservation and modulation of hepatocyte phenotypes. Using our hybrid co-culture model, we observed that the contact of hepatocytes with endothelial cells appeared to stimulate higher hepatic-specific gene expression as compared to that achieved in the monoculture system. Furthermore, urea production was elevated in the co-cultures and was maintained at higher levels throughout the whole culture period (Fig. 6). These results are consistent with other culture models that used different materials (24—26). Although the precise mechanisms regulating increases in liver-specific hepatocyte functions in co-culture systems have not been elucidated, the likely mediators of cell—cell communication (secreted and/or cell-associated signals) could affect the stabilization and the enhancement of cell functionality. Future studies will be devoted to uncovering the mechanisms at work in this system, including the signals transmitted between the hepatocytes and endothelial cells.

In summary, the highly porous GCs/HA-hybrid sponge provided an ECM-like environment that was suitable for the co-culture of hepatocytes and endothelial cells. This biocompatible hepatocyte/endothelial hybrid scaffold may be a suitable storage and delivery vehicle for transplantation and holds promise towards the development of a bioengineered artificial liver system.

Supplementary data related to this article can be found at http://dx.doi.org/10.1016/j.jbiosc.2013.06.015.

ACKNOWLEDGMENTS

This study was supported by a Grant-in-Aid for Challenging Exploratory Research (no. 24650254) from the Japan Society for the Promotion of Science (JSPS) and a Grant-in-Aid for Scientific Research on Innovative Areas (no. 231190003) from the Ministry of Education, Culture, Sports, Science and Technology (MEXT) of Japan. Yi Shang received the MEXT Scholarship from Japanese Government. We also thank all members of our laboratory for their excellent animal care.

References

1. **Ogawa, S., Tagawa, Y., Kamiyoshi, A., Suzuki, A., Nakayama, J., Hashikura, Y., and Miyagawa, S.:** Crucial roles of mesodermal cell lineages in a murine embryonic stem cell-derived in vitro liver organogenesis system, Stem Cells, **23**, 903—913 (2005).
2. **Tamai, M., Yamashita, A., and Tagawa, Y.:** Mitochondrial development of the in vitro hepatic organogenesis model with simultaneous cardiac mesoderm differentiation from murine induced pluripotent stem cells, J. Biosci. Bioeng., **112**, 495—500 (2011).
3. **Tsutsui, M., Ogawa, S., Inada, Y., Tomioka, E., Kamiyoshi, A., Tanaka, S., Kishida, T., Nishiyama, M., Murakami, M., Kuroda, J., and other 5 authors:** Characterization of cytochrome p450 expression in murine embryonic stem cell-derived hepatic tissue system, Drug Metab. Dispos., **34**, 696—701 (2006).
4. **Toyoda, Y., Tamai, M., Kashikura, K., Kobayashi, S., Fujiyama, Y., Soga, T., and Tagawa, Y.:** Acetaminophen-induced hepatotoxicity in a liver tissue model consisting of primary hepatocytes assembling around an endothelial cell network, Drug Metab. Dispos., **40**, 169—177 (2011).
5. **Banerji, S., Wright, A. J., Noble, M., Mahoney, D. J., Campbell, I. D., Day, A. J., and Jackson, D. G.:** Structures of the Cd44-hyaluronan complex provide insight into a fundamental carbohydrate-protein interaction, Nat. Struct. Mol. Biol., **14**, 234—239 (2007).
6. **McDonald, B., McAvoy, E. F., Lam, F., Gill, V., de la Motte, C., Savani, R. C., and Kubes, P.:** Interaction of CD44 and hyaluronan is the dominant mechanism for neutrophil sequestration in inflamed liver sinusoids, Jpn. J. Exp. Med., **205**, 915—927 (2008).
7. **Misra, S., Heldin, P., Hascall, V. C., Karamanos, N. K., Skandalis, S. S., Markwald, R. R., and Ghatak, S.:** Hyaluronan-CD44 interactions as potential targets for cancer therapy, FEBS J., **278**, 1429—1443 (2011).
8. **Park, I.-K., Yang, J., Jeong, H.-J., Bom, H.-S., Harada, I., Akaike, T., Kim, S.-I., and Cho, C.-S.:** Galactosylated chitosan as a synthetic extracellular matrix for hepatocytes attachment, Biomaterials, **24**, 2331—2337 (2003).
9. **Ryu, J.-Y., Siswanto, A., Harimoto, K., and Tagawa, Y.:** Chimeric analysis of EGFP and DsRed2 transgenic mice demonstrates polyclonal maintenance of pancreatic acini, Transgenic Res., **22**, 549—556 (2012).
10. **Selgen, P. O.:** Preparation of isolated rat liver cells, Methods Cell Biol., **13**, 29—83 (1976).
11. **Edgell, C., Mcdonald, C., and Graham, J.:** Permanent cell line expressing human factor VIII-related antigen established by hybridization, Proc. Natl. Acad. Sci. USA, **80**, 3734—3737 (1983).
12. **Wang, L. and Stegemann, J. P.:** Extraction of high quality RNA from polysaccharide matrices using cetyltrimethylammonium bromide, Biomaterials, **31**, 1612—1618 (2010).
13. **Hoshiba, T., Nagahara, H., Cho, C.-S., Tagawa, Y., and Akaike, T.:** Primary hepatocyte survival on non-integrin-recognizable matrices without the activation of Akt signaling, Biomaterials, **28**, 1093—1104 (2007).
14. **Cho, C. S., Seo, S. J., Park, I. K., Kim, S. H., Kim, T. H., Hoshiba, T., Harada, I., and Akaike, T.:** Galactose-carrying polymers as extracellular matrices for liver tissue engineering, Biomaterials, **27**, 576—585 (2006).

15. **Feng, Z.-Q., Chu, X., Huang, N.-P., Wang, T., Wang, Y., Shi, X., Ding, Y., and Gu, Z.-Z.:** The effect of nanofibrous galactosylated chitosan scaffolds on the formation of rat primary hepatocyte aggregates and the maintenance of liver function, Biomaterials, **30**, 2753–2763 (2009).
16. **Nagaoka, M., Koshimizu, U., Yuasa, S., Hattori, F., Chen, H., Tanaka, T., Okabe, M., Fukuda, K., and Akaike, T.:** E-cadherin-coated plates maintain pluripotent ES cells without colony formation, PLoS One, **20**, e15 (2006).
17. **Bierwolf, J., Lutgehetmann, M., Feng, K., Erbes, J., Deichmann, S., Toronyi, E., Stieglitz, C., Nashan, B., Ma, P. X., and Pollok, J. M.:** Primary rat hepatocyte culture on 3D nanofibrous polymer scaffolds for toxicology and pharmaceutical research, Biotechnol. Bioeng., **108**, 141–150 (2011).
18. **Skardal, A., Smith, L., Bharadwaj, S., Atala, A., Soker, S., and Zhang, Y.:** Tissue specific synthetic ECM hydrogels for 3-D in vitro maintenance of hepatocyte function, Biomaterials, **33**, 4565–4575 (2012).
19. **Lau, T. T., Lee, L. Q. P., Leong, W., and Wang, D.-A.:** Formation of model hepatocellular aggregates in a hydrogel scaffold using degradable genipin crosslinked gelatin microspheres as cell carriers, Biomed. Mater., **7**, 065003 (2012).
20. **Fan, J., Shang, Y., Yuan, Y., and Yang, J.:** Preparation and characterization of chitosan/galactosylated hyaluronic acid scaffolds for primary hepatocytes culture, J. Mater. Sci. Mater. Med., **21**, 319–327 (2009).
21. **Zhu, X. H., Lee, L. Y., Jackson, J. S. H., Tong, Y. W., and Wang, C.-H.:** Characterization of porous poly(D,L-lactic-co-glycolic acid) sponges fabricated by supercritical CO_2 gas-foaming method as a scaffold for three-dimensional growth of Hep3B cells, Biotechnol. Bioeng., **100**, 998–1009 (2008).
22. **Guy, C. S., Rankin, S. L., and Michalak, T. I.:** Hepatocyte cytotoxicity is facilitated by asialoglycoprotein receptor, Hepatology, **54**, 1043–1050 (2011).
23. **Soenen, S. J. H., Brisson, A. R., Jonckheere, E., Nuytten, N., Tan, S., Himmelreich, U., and De Cuyper, M.:** The labeling of cationic iron oxide nanoparticle-resistant hepatocellular carcinoma cells using targeted magnetoliposomes, Biomaterials, **32**, 1748–1758 (2011).
24. **Inamori, M., Mizumoto, H., and Kajiwara, T.:** An approach for formation of vascularized liver tissue by endothelial cell-covered hepatocyte spheroid integration, Tissue Eng. Part A, **15**, 2029–2037 (2009).
25. **Salerno, S., Campana, C., Morelli, S., Drioli, E., and De Bartolo, L.:** Human hepatocytes and endothelial cells in organotypic membrane systems, Biomaterials, **32**, 8848–8859 (2011).
26. **Wen, F., Chang, S., Toh, Y. C., Arooz, T., Zhuo, L., Teoh, S. H., and Yu, H.:** Development of dual-compartment perfusion bioreactor for serial coculture of hepatocytes and stellate cells in poly(lactic-co-glycolic acid)-collagen scaffolds, J. Biomed. Mater. Res. Part B Appl. Biomater., **87B**, 154–162 (2008).

TISSUE ENGINEERING: Part A
Volume 19, Numbers 21 and 22, 2013
© Mary Ann Liebert, Inc.
DOI: 10.1089/ten.tea.2012.0704

Characterization of a Liver Organoid Tissue Composed of Hepatocytes and Fibroblasts in Dense Collagen Fibrils

Miho Tamai, DEng,[1] Eijiro Adachi, MD, PhD,[2] and Yoh-ichi Tagawa, DSc[1]

The adult liver is wrapped in a connective tissue sheet called the liver capsule, which consists of collagen fibrils and fibroblasts. In this study, we set out to construct a liver organoid tissue that would be comparable to the endogenous liver, using a bioreactor. *In vitro* liver organoid tissue was generated by combining collagen fibrils, fibroblasts, and primary murine hepatocytes or Hep G2 on a mesh of poly-lactic acid fabric using a bioreactor. Then, the suitability of this liver organoid tissue for transplantation was tested by implanting the constructs into partially hepatectomized BALB/cA-nu/nu mice. As determined by using scanning and transmission electron microscopes, the liver organoid tissues were composed of densely packed collagen fibrils with fibroblasts and aggregates of oval or spherical hepatocytes. Angiogenesis was induced after the transplantation, and blood vessels connected the liver organoid tissue with the surrounding tissue. Thus, a novel approach was applied to generate transplantable liver organoid tissue within a condensed collagen fibril matrix. These results suggested that a dense collagen network populated with fibroblasts can hold a layer of concentrated hepatocytes, providing a three-dimensional microenvrionment suitable for the reestablishment of cell–cell and cell–extracellular matrix (ECM) interactions, and resulting in the maintenance of their liver-specific functions. This liver organoid tissue may be useful for the study of intrahepatic functions of various cells, cytokines, and ECMs, and may fulfill the fundamental requirements of a donor tissue.

Introduction

Extracellular matrices (ECMs) provide structural support for cells and perform various important functions. Collagens, a family of fibrous proteins, are the most abundant proteins in the ECM.[1] The collagens are secreted by a variety of cell types, especially by connective tissue cells.

The adult liver is wrapped in a connective tissue sheet named the liver capsule, which consists of collagen fibrils and fibroblasts.[2] A great deal of research has been focused on the maintenance of hepatocyte functions *in vitro*. Primary hepatocytes have been cultured on biomaterials *in vitro*, for example, collagen gels,[3–6] Engelbreth–Holm–Swarm gels,[7–9] and other materials.[10–13] There are also some recent studies using collagen sandwich hepatocyte cultures that have achieved long culture periods and the maintenance of hepatic functions.[14–16] However, no studies have described the reconstruction of highly concentrated connective tissue *in vitro* with properties similar to endogenous liver tissue. In the liver, type I collagen fibrils serve as a primary scaffold upon which are deposited microfibrils and filaments of collagen types III, V, and VI.[17,18] To construct useful *in vitro* liver models, it is very important to form collagen fibrils in the connective tissue. Recently, it has become possible to stably construct a fibroblast-embedded condensed collagen fibril layer using a closed loop system composed of three major parts: a reservoir bottle, a diaphragm pump, and a bioreactor chamber.[19] Because fibroblasts are embedded in the network collagen fibrils of this artificial tissue, it is useful for reconstructing the hepatic interstitial structure. Here, we constructed a liver organoid tissue using an originally designed bioreactor system, and implanted this tissue into the nude mouse.

Materials and Methods

Animals

Male C57BL/6JJcl mice, 6–8 weeks old (20–25 g; CLEA Japan, Tokyo, Japan), were used for hepatocyte isolation. Pregnant female ICR mice at 13 days postcoitus (CLEA Japan) were used for embryonic fibroblast isolation. Female BALB/cAJcl-nu/nu mice, 6 weeks old (17–18 g; CLEA Japan), were used as reconstructive hepatic transplant recipients. The animal protocols were approved by the Animal Experimentation Committee of Tokyo Institute of Technology.

[1]Department of Biomolecular Engineering, Graduate School of Bioscience and Biotechnology, Tokyo Institute of Technology, Kanagawa, Japan.
[2]Department of Molecular Morphology, Kitasato University Graduate School of Medical Sciences, Kanagawa, Japan.

Cell lines

The human hepatocellular carcinoma cell line, Hep G2, was provided by the RIKEN Bio-Resource Center (Tsukuba, Japan). Human diploid fibroblast, HFO, was provided by Dr. Satoshi Amano (Shiseido Institute, Shiseido, Tokyo, Japan). Both cell types were cultured in the Dulbecco's modified Eagle's medium (DMEM; Invitrogen, Tokyo, Japan) containing 10% fetal bovine serum (FBS; Nichirei Biosciences, Tokyo, Japan) under 5% CO_2 at 37°C. These cells were subcultured by treatment with 0.05% trypsin (Invitrogen) and 20 μM ethylenediaminetetraacetic acid (EDTA; Nacalai Tesque, Kyoto, Japan).

Isolation of murine hepatocytes

Hepatocytes were prepared from anesthetized BALB/cA mice by a two-step *in situ* collagenase perfusion method,[20] with slight modifications. Briefly, murine liver was preperfused *in situ* with Hank's balanced salt solution (HBSS) containing 0.5 mM ethylene glycol tetraacetic acid (EGTA). Next, the liver was perfused with 0.015% collagenase in HBSS. Then, the liver was removed, and the cells were dispersed in ice-cold HBSS without EGTA. The resulting cells were filtered through a 100-μm-pore mesh nylon cell strainer (BD Biosciences, MA) and centrifuged twice for 2 min at 500 *g* to remove nonparenchymal cells. The remaining cells were centrifuged for 2 min at 500 *g*, and then subjected to a 40% Percoll density gradient centrifugation for 10 min at 1200 *g*. At this stage, cell viability as measured by trypan blue was >90%. The isolated hepatocytes were plated at a density of 1.2×10^6 cells per well in collagen-coated six-well plates. Cells were grown in the high-glucose (25 mM) DMEM (Invitrogen) containing 10% (v/v) heat-inactivated FBS, 100 U/mL penicillin, and 100 μg/mL streptomycin (Invitrogen) at 37°C in a humidified incubator with 5% CO_2. The medium was changed after the first 4 h of incubation, and was replaced daily thereafter.

Preparation of murine embryonic fibroblasts

A pregnant female ICR at 13.5 days postcoitum was sacrificed by cervical dislocation, and embryos were removed. The limbs of the embryos were minced and treated with 0.25% trypsin (Invitrogen) + 1 mM EDTA (~2 mL per embryo) and incubated with gentle stirring at 37°C for 10–15 min. The recovered cells were subsequently cultured in the DMEM containing 10% (v/v) FBS.

Establishment of DsRed-expressing Hep G2

Hep G2 cells were cultured in the DMEM supplemented with penicillin/streptomycin and 10% (v/v) FBS. The CAG promoter-driven DsRed2 expression vector was constructed by subcloning the 1.7-kb *Sal* I-CAG promoter-*EcoR* I fragment from pCAGGS into the corresponding site of the pDsRed2-1 vector in the sense orientation.[21] Twenty-five micrograms of CAG-DsRed2-1/*EcoR* I were transfected into human hepatocellular carcinoma cells by electroporation (1×10^7 cells; 230 V; 500 μF; 0.4 cm electrode gap). After electroporation, the cells were plated in 100-mm dishes. Selection was initiated the next day by adding 3 mg/mL G-418 to the culture medium. Clones of human hepatocellular carcinoma cells transfected with CAG-DsRed2-1/*EcoR* I were selected and maintained, and DsRed2 expression in these cells was assessed by flow cytometry. The highly fluorescent clones were isolated as Hep G2^{Red} cells and used in transplantation experiments.

Generation of structural liver organoid tissue

As can be seen in Figure 1, structural liver organoid tissue was generated by combining collagen fibrils, primary murine embryonic fibroblasts, and primary murine hepatocytes or Hep G2^{Red} cells *in vitro* using a closed-loop system within a bioreactor chamber (diameter 17 mm × height 20 mm) developed by our group.[19] We circulated 42.5 mL of 10% FBS/DMEM, supplemented with 7.5 mL of 50 mg/mL type I collagen prepared from calf skin by pepsin treatment (Koken Collagen, Tokyo, Japan), through the closed-loop system for 3 h. Then, we used a syringe to inject primary murine embryonic fibroblasts (5.0×10^6 cells suspended in 2 mL 10% FBS/DMEM, high glucose) into the system upstream of the bioreactor chamber. The mixed solution flowed through the closed-loop system at a predetermined flow rate (1–5 mL/min) for 6 h. Subsequently, 50 mL of 10% FBS/DMEM was circulated through the closed-loop system, and primary murine hepatocytes (1.0×10^7 cells suspended in 2 mL 10% FBS/DMEM) were injected into the system upstream of the bioreactor chamber. After 2 h, 42.5 mL of 10% FBS/DMEM, supplemented with 7.5 mL of 50 mg/mL type I collagen prepared from calf skin by pepsin treatment, was circulated through the closed-loop system for 3 h, and primary murine embryonic fibroblasts (5.0×10^6 cells suspended in 2 mL 10% FBS/DMEM) were injected into the system upstream of the bioreactor chamber.

Morphological analyses

The liver organoid tissue was fixed with Zamboni's fixative for light microscopy, scanning and transmission electron microscopy. For light microscopy, the samples were dehydrated with an ethanol series and embedded in paraffin. The sections were stained with hematoxylin and eosin and examined with a light microscope. The samples were post-fixed with 2% osmium tetroxide in 0.1 M phosphate buffer, processed routinely, and ultimately examined with a scanning electron microscope (JSM 6360; JEOL Co., Ltd., Tokyo, Japan) or a transmission electron microscope (H8100; Hitachi Co., Ltd., Tokyo, Japan).

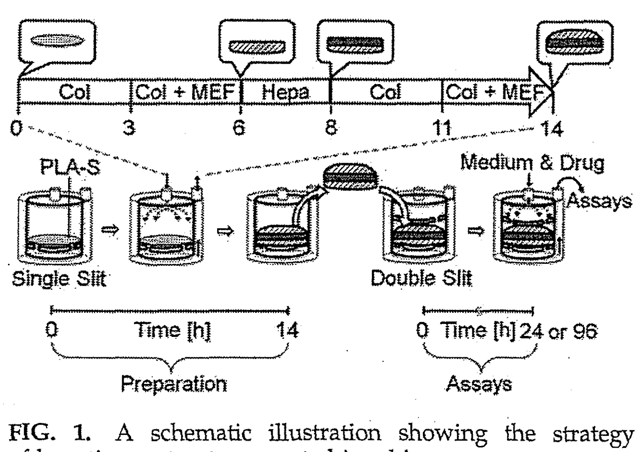

FIG. 1. A schematic illustration showing the strategy of hepatic constructs generated in a bioreactor.

Hepatic function assays in liver organoid tissue

Urea production in the conditioned medium, 24 h after the addition of 2 mM ammonium chloride (NH_4Cl; Sigma-Aldrich Japan, Tokyo, Japan) was quantified using a urea assay kit (Bioassay Systems, Hayward, CA). Albumin production in the conditioned medium was quantified using the Albuwell M albumin EIA kit (Exocell, Philadelphia, PA).

Testosterone metabolites in the conditioned medium were quantified by high performance liquid chromatography (HPLC) analysis.[22] The liver organoid tissue was incubated with a fresh medium containing 0.25 mM testosterone for 24 h. Next, the conditioned medium was collected and mixed with 5 mL of ethyl acetate and 1 μL of 2.5 mM 11α-hydroxy-progesterone/dimethyl sulfoxide. After centrifugation, the organic layer was evaporated to prepare the HPLC sample. HPLC analysis was performed using LC-10ADVP (Shimadzu, Kyoto, Japan) with Cadenza columns (Cadenza CD-C18; Imtakt, Kyoto, Japan) and SPD-10A VP (Shimadzu). Testosterone hydroxylation was assessed using the C-R8A software (Shimadzu).

Transplantation of liver organoid tissue

While under pentobarbital anesthesia, the mice were subjected to an upper abdominal incision, and then the right portal vein branch was exposed and ligated, and the right lobes of the liver (30%) were hepatectomized. Then, the liver organoid tissue was transplanted into the mice. Two weeks later, the intraperitoneal liver organoid tissue was removed for histological analysis of the vascular network or transplanted hepatocytes at the same location.

Statistical evaluation

Results of multiple experiments ($n = 3$–4) are reported as the mean ± standard error (SE). Statistical comparisons were made using a Student's *t*-test.

Results

Three-dimensional reconstruction of hepatic tissue using a bioreactor

A solution of type I collagen and primary murine embryonic fibroblasts was introduced into a bioreactor via a closed-loop system, followed by the sequential addition of primary murine hepatocytes and a second round of collagen and primary murine embryonic fibroblasts. These manipulations produced a hepatic aggregate consisting of a layer of primary hepatocytes sandwiched between two layers of embryonic fibroblasts and deposited collagen fibrils on a sheet of poly-lactic acid (PLA). Glossy aggregates had accumulated on the PLA sheet after 14 h of circulation through the bioreactor (Fig. 1). The dissolved oxygen content was 5.16 ± 0.07 mg/L at the outlet of the circulating medium.

The liver organoid tissue was 1.5 mm in thickness and 17 mm in diameter (Fig. 2A, B). The average weight of the organoid tissue was ~0.4 g. Further, the density of the collagen layer was 34 ± 2.5 mg/cm^2, which is almost same as that of endogenous murine connective tissue.

Morphological analysis of hepatocytes in the liver organoid tissue

Cross-sectional profiles of the liver organoid tissue were stained with hematoxylin and eosin (Fig. 2C). Clusters of hepatocytes were sandwiched between two layers of collagen fibrils populated with murine fibroblasts. We could clearly see a layer of primary hepatocytes ~200–500 μm thick, and two layers of collagen fibrils populated with embryonic fibroblasts, ~300–500 μm thick. Upon close inspection, round or spherical hepatocytes, ~20 μm in diameter, were seen on collagen fibers, while fibroblasts tended to be bipolar or stellate in shape within the layers of collagen fibrils (Fig. 2D).

The liver organoid tissue was examined by scanning electron microscopy to investigate the extracellular microenvironment of the hepatocytes. The collagen layers were composed of densely packed collagen fibrils running parallel to the plane of the PLA sheet in the three-dimensional (3D) culture. Primary hepatocytes were oval or spherical in shape and formed clusters. By contrast, hepatocytes cultured in two dimensions (2D) on collagen-coated dishes were generally flat, and displayed lamellipodia after 3 days (Fig. 3A). These results suggest that the layers of collagen fibrils played an important role in establishing or maintaining the globular morphology of hepatocytes in the 3D microenvironment (Fig. 3B).

Under a transmission electron microscope, we could observe clusters of primary hepatocytes (Fig. 4). They had a round nucleus characterized by an irregular contour (Fig. 4A). In the hepatocyte cytoplasm, we could identify several mitochondria with cristae, 0.2–0.6 μm in diameter, and a small Golgi apparatus composed of five to seven

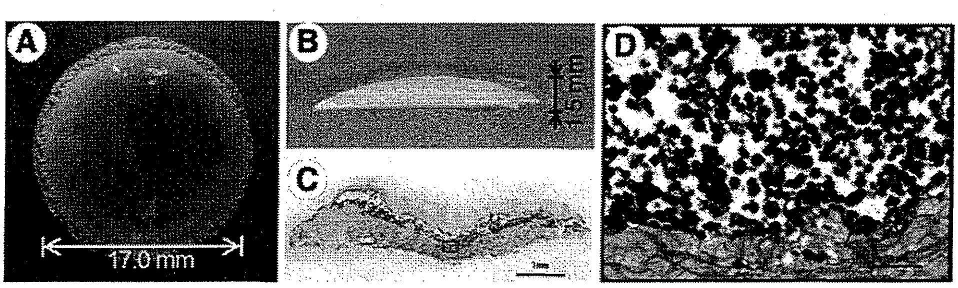

FIG. 2. Micrographic observations of liver organoid tissue. **(A)** Top view of a whole liver organoid tissue construct. The glossy and reddish organoid tissue is discoidal. **(B)** Cross-sectional profile of an organoid tissue construct. **(C, D)** Cross sections were stained with hematoxylin and eosin. **(C)** A hepatic cell mass is sandwiched between two layers of collagen fibrils populated with fibroblasts. **(D)** Light micrograph showing an inscribed area in **(C)**. Primary hepatocytes are round and ~20 μm in diameter. The scale bars correspond to 1 mm **(C)** and 50 μm **(D)**. Color images available online at www.liebertpub.com/tea

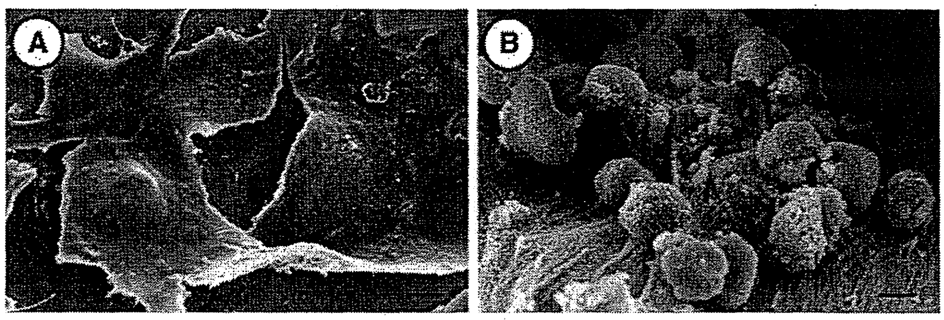

FIG. 3. Scanning electron micrographic observations of primary hepatocytes on a collagen-coated dish (two dimensional [2D]) or in the liver organoid tissue (three dimensional [3D]). Hepatocytes cultured on collagen-coated dishes **(A)** and in liver organoid tissue **(B)**. The scale bar corresponds to 10 μm.

flattened cisternae. We also encountered flattened endoplasmic reticula in the peripheral region of primary hepatocytes. A limited number of collagen fibrils approached the primary hepatocytes and appeared to attach to their surface (Fig. 4B). In the cluster of hepatocytes, numerous channels resembling bile canaliculi could be observed between neighboring cells (Fig. 4C–E). The size of these channels varied from 0.2 to 0.5 μm wide. They had short microvilli, 0.1–0.2 μm long, protruding into the lumen. Frequently, the cell membranes were more closely apposed than usual. Adherent junctions and gap junctions were commonly observed in the vicinity of bile canaliculi, but tight junctions were rarely seen.

Structural liver organoid tissue exhibits multiple liver-specific functions

Several liver-specific functions, for example, the production of urea and albumin and drug metabolism activity, were analyzed in the liver organoid tissue. Ammonia, which is toxic to the central nervous system, may be detoxified into urea through the coordinated actions of the urea cycle in hepatocytes. Therefore, we investigated urea production as a liver-specific function that is mediated in the mitochondria and cytoplasm of hepatocytes. To investigate the potential for dynamic urea synthesis, the urea concentrations were measured in liver organoid tissue conditioned media after

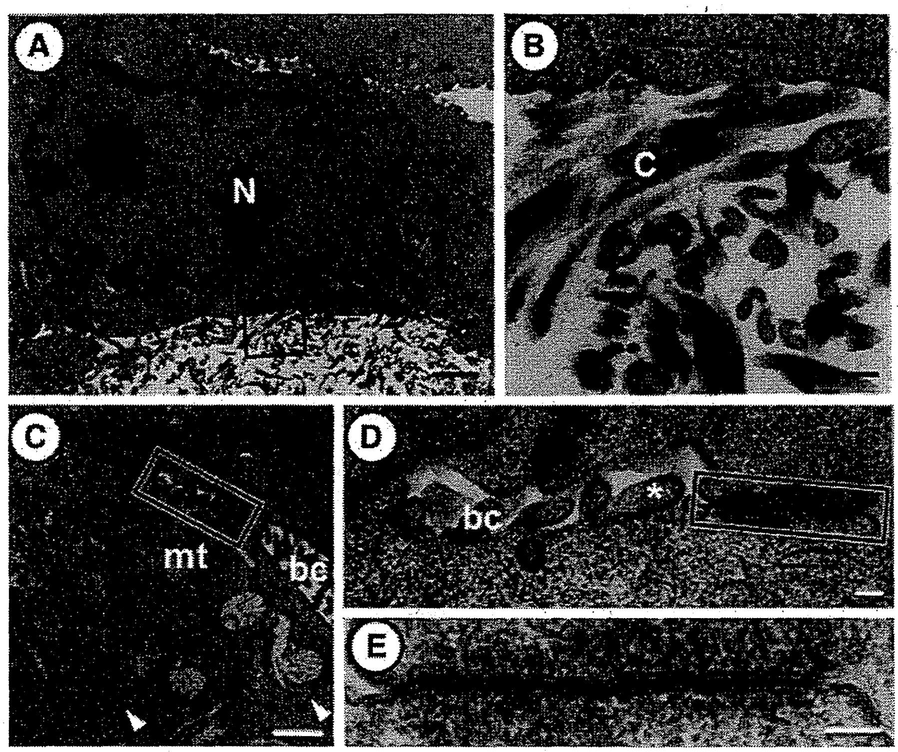

FIG. 4. Transmission electron micrographs showing primary hepatocytes in liver organoid tissue. **(A)** The cells are ~15 μm wide, spherical in shape, and have a prominent cytoplasm containing mitochondria and endoplasmic reticulum. **(B)** Higher magnification of the inscribed area in **(A)**. Collagen fibrils appear to be attached to the cell surface. **(C–E)** Transmission electron micrographs showing the cytoplasm **(C)**, bile canaliculi **(C, D)**, and a gap junction **(E)** between the neighboring cells. **(C)** In the cytoplasm, mitochondria with cristae and endoplasmic reticulum (arrowheads) can be observed. Tubular bile canaliculi are frequently observed between the cells. **(D)** Higher magnification of the inscribed area in **(C)**. Short microvilli (asterisk) protrude into the lumen of the bile canaliculi. **(E)** Higher magnification of the inscribed area in **(D)**. The cell membranes are closely apposed to form a gap junction. The scale bars correspond to 1 μm **(A)**, 100 nm **(B)**, 1 μm **(C)**, and 100 nm **(D, E)**. Abbreviations: mt, mitochondria; bc, bile canaliculi; C, collagen fibril; N, nuclei.

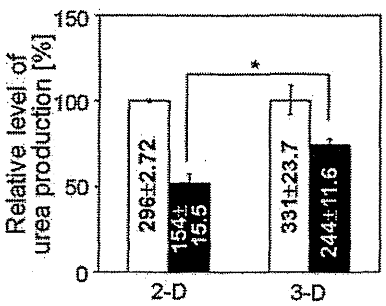

FIG. 5. Urea concentrations in the conditioned medium of 2D (collagen-coated dishes) and 3D (liver organoid tissue) hepatocyte cultures. The relative amount of urea in the conditioned media after 72 h was calculated by setting the values obtained at 24 h to 100%. The absolute values (μg/10^6 cells) are noted in the corresponding columns. Mean ± standard error (SE), $n=3$; $^*p<0.01$.

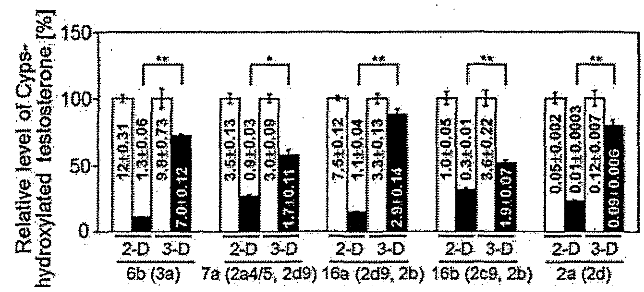

FIG. 7. Testosterone hydroxylation in 2D (collagen-coated dishes) and 3D (liver organoid tissue) hepatocyte cultures. The relative amount of each hydroxylated testosterone was calculated by setting the values obtained at 24 h to 100%. The absolute values (nmol/10^6 cells) are noted in the corresponding columns. Mean ± SE, $n=3$; $^*p<0.05$; $^{**}p<0.01$.

the addition of NH_4Cl (Fig. 5). Urea production was observed in the liver organoid tissue after the addition of the ammonium ion. We compared the functional activity of the liver organoid tissue to that in 2D hepatocyte cultures, and observed that urea production in the former was significantly higher at 72 h than in the latter, suggesting that liver organoid tissue culture can maintain hepatic functions that are lost or impaired in 2D cultures.

We also measured the levels of albumin secretions in the conditioned media from the liver organoid tissues or 2D hepatocyte cultures. A measurable amount of albumin was synthesized in the organoid tissues. The level of albumin production in the organoid tissue was well maintained; specifically, the levels on day 3 were ~85% of those observed on day 1. The values obtained in the 2D cultures indicated a steeper drop in albumin production over time for the cells cultured on collagen alone (Fig. 6).

Many poisonous compounds in the blood enter hepatocytes through various mechanisms, including endocytosis and passive diffusion. These compounds may be metabolized in the microsomal system, which includes the cytochrome P450 (CYP450) enzymes. We tested the activities of the CYP450 enzymes in the liver organoid tissue and in 2D hepatocyte cultures. Specifically, we measured the testosterone oxidation patterns in the organoid tissue-conditioned media using high-performance liquid chromatography. We quantified the concentration of each hydroxylated testosterone: 15α-OHT, 6β-OHT, 7α-OHT, 16α-OHT, 16β-OHT, 2α-OHT, and 2β-OHT, corresponding to oxidation by Cyp2a4/5, Cyp3a, Cyp2a4/5 and 2d9, Cyp2d9 and 2b, Cyp2c29 and 2b, and Cyp2d, respectively. The concentrations of hydroxylated testosterones, for example, 6β-OHT, 7α-OHT, 16α-OHT, and 16β-OHT, in the organoid tissue conditioned media on day 3 were ~50%–70% of those observed on day 1. These results indicate that the organoid tissues maintained 50%–70% of their cytochrome P450 enzyme activity after 3 days in culture. By contrast, the concentrations of hydroxylated testosterones on day 3 of the 2D culture were <25% of those recorded on day 1 (Fig. 7).

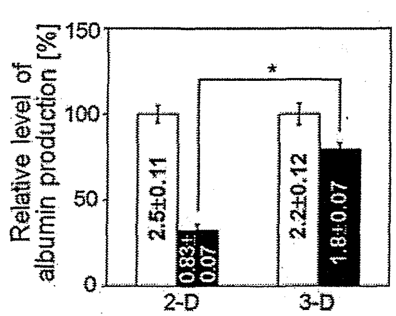

FIG. 6. Albumin concentrations in the conditioned medium of 2D (collagen-coated dishes) and 3D (liver organoid tissue) hepatocyte cultures. The relative amount of albumin in the conditioned media after 72 h was calculated by setting the values obtained at 24 h to 100%. The absolute values (μg/10^6 cells) are noted in the corresponding columns. Mean ± SE, $n=3$; $^*p<0.01$.

Hep G2/HFO liver organoid tissue was successfully engrafted in a partially hepatectomized nude mouse

In addition to the experiments using primary murine hepatocytes, we also prepared liver organoid tissue using Hep G2, a human hepatocellular carcinoma cell line, for use in transplantation experiments (Fig. 8A). To easily discriminate the donor cells from the recipient cells in the engrafted area, a DsRed2 expression vector was introduced into the Hep G2 cells and the vector integrated into the genomic DNA. Seven clones that consistently expressed high levels of DsRed2, as determined by flow cytometry, were obtained. A clone that had 100% $DsRed2^+$ progeny was designated Hep $G2^{Red}$ (Fig. 8B, C) and used for the following experiments. A liver organoid tissue was generated consisting of Hep $G2^{Red}$, in place of primary hepatocytes, and HFO, a human fibroblast cell line, in place of primary fibroblasts. The Hep $G2^{Red}$/HFO liver organoid tissue was ~1.6 mm in thickness and 17 mm in diameter. This liver organoid tissue was ectopically transplanted into the peritoneal cavity of a female BALB/cA-*nu/nu* mouse after a partial hepatectomy (Fig. 8A). The graft could be observed in the peritoneal cavity 2 weeks after transplantation. Microvascular networks could be observed throughout this engrafted tissue (Fig. 8D). We prepared 4-μm sections of the graft treated with Zamboni's fixation. The AZAN staining of this specimen showed that collagen remained abundant in the graft, that fibroblasts existed

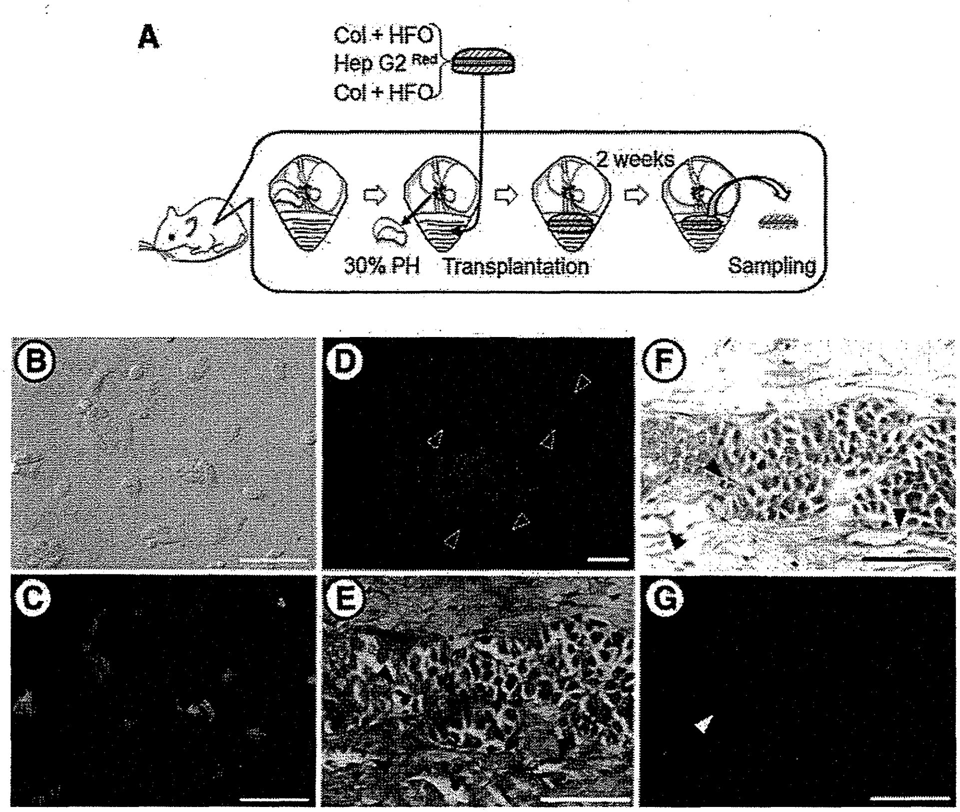

FIG. 8. Transplanted liver organoid tissues in a partially hepatectomized mouse model. **(A)** A schematic illustration showing the transplantation of liver organoid tissue. Light micrograph **(B)** and fluorescent micrograph **(C)** images of transplanted DsRed2-expressing Hep G2 cells. **(D–G)** Micrographs of liver organoid tissue. **(D)** Fluorescent image. The red fluorescence indicates surviving DsRed-expressing Hep G2^{Red} cells. Arrowheads indicate new blood vessels, which appear black. **(E, F)** Histological analyses: AZAN and hematoxylin–eosin staining, respectively, of liver organoid tissue sections after transplantation. Vascularization was detected at the condensed collagen fibril matrices. Arrowheads indicate new blood vessels. **(G)** Immunohistochemical analysis of the transplanted hepatic construct indicting albumin-positive hepatic cells and CD31/PECAM-1-positive endothelial cells using anti-albumin (red) and anti-CD31/PECAM-1 (green) antibodies. Arrowheads indicate new blood vessels. The scale bar corresponds to 200 μm. The animal transplantation experiments were carried out four times. Color images available online at www.liebertpub.com/tea

within the collagen, and that vessel-like tube formation could be observed in both the collagen and the Hep G2^{Red} areas (Fig. 4E). Next, hematoxylin–eosin staining and immunohistochemical examination with anti-albumin and anti-CD31/PECAM-1 antibodies were performed (Fig. 8F, G, respectively). Endothelial cells, CD31+ cells, formed a tube-like structure in the albumin-positive region of the graft (Fig. 8G). These results indicate that the Hep G2^{Red}/HFO liver organoid tissue was successfully engrafted and vascularized in the partially hepatectomized nude mouse.

Discussion

Primary cultured hepatocytes have been extensively used as a model system for pharmacological, toxicological, and metabolic studies; however, the metabolism and gene expression patterns of primary cultured cells are frequently altered during culture in a 2D system, which in turn is influenced by changes in cellular morphology, intercellular signal transduction, and other extracellular environmental cues.[23,24] Cells in tissues and organs exist in a 3D environment surrounded by other cells. The cuboidal cell shape, distinct polarity, and 3D cellular communication are known to be crucial for key metabolic pathways and tissue-specific phenotypes. Novel *in vitro* culture systems that more authentically represent the cellular environment are required for advancing our understanding of complex biological phenomena.

Ten million hepatocytes were entrapped between two layers of collagen fibrils populated with fibroblasts using a bioreactor that we designed. Hepatocytes cultured as liver organoid tissue maintained urea and albumin synthesis and the CYP450 activity significantly better than hepatocytes cultured on collagen-coated dishes. Morphologically, hepatocytes in the liver organoid tissue were oval or spherical in shape and ~15 μm in diameter. Hepatocytes in the liver organoid tissue formed clusters that were surrounded by a network of densely packed collagen fibrils. A limited number of collagen fibrils approached the hepatocytes and appeared to be anchored to their surface. Therefore, these hepatocytes could interact with collagen fibrils through integrins. Collagen fibrils may offer scaffolds for hepatocytes and may alter their behavior, including their growth, viability, and liver-specific functions.

There are several reports describing collagen sandwich hepatocyte monolayer cultures that demonstrate the maintenance of hepatic functions and long culture periods (8 days). Dunn *et al.* showed that the hepatocyte morphology under collagen-sandwich culture conditions was normal.[5] In this report, we showed that after 3 days in culture, the hepatocytes still had a round shape, resembling their endogenous counterparts (Fig. 3). It is considered to be structurally impossible to have a bile canaliculi in the context of a 2D culture; by contrast, we observed a bile canaliculi in our 3D system (Fig. 4C, D). Thus, three dimensions are needed to form a bile canaliculi.

Hepatocytes in 3D cultures had oval nuclei with irregular contours and larger amounts of cytoplasm as compared to those in 2D cultures. This observation suggests that hepatocytes in the organoid tissue contained more organelles, for example, mitochondria, Golgi apparatus, and endoplasmic reticula, than those on culture dishes. Between the hepatocytes, we could frequently observe bile canaliculi and cell–cell junctions, resembling adherent and gap junctions. The bile canaliculi in the liver organoid tissue were 0.5–1.0 μm wide, and short microvilli protruded into their lumen. The formation of bile canaliculi in artificial liver tissues has also been reported elsewhere.[3,25] Bile acid excretion is considered to be one of the primary detoxification mechanisms in the liver, because the accumulated bile acids in hepatocytes may provide detergent effects on the cell membrane. Based on these morphological findings, primary hepatocytes entrapped between the collagen networks can restore the polarization of hepatocytes *in vivo*.

Many reports suggest that liver-specific functions could be maintained by a 3D organization, cell density,[17,26] and interaction with ECM.[4,5] The liver organoid tissue generated in our bioreactor could serve as artificial liver tissue demonstrating strong hepatic differentiated functions, for example, the expression of *albumin*, *tyrosine amino transferase*, *transthyretin*, and *tryptophan 2, 3-dioxygenase* (data not shown). We also confirmed that urea synthesis could be maintained in liver organoid tissues, probably because stacked hepatocytes possessed a large amount of cytoplasm and mitochondria.

Testosterone is metabolized in a region-selective manner by different P450 enzymes, and can be used as a multienzymatic substrate to simultaneously investigate the activities of multiple enzymes. The testosterone hydroxylation system is localized in the endoplasmic reticulum. In this study, we noted that the testosterone hydroxylation activity was maintained in the liver organoid tissue hepatocytes after 3 days in culture. It is conceivable that oval or spherical hepatocytes in the liver organoid tissues could maintain a considerable amount of endoplasmic reticulum in their cytoplasm, because the average volume of oval hepatocytes should be greater compared with flattened cells on culture dishes.

One of the major objectives in using liver organoid tissue for hepatocyte transplantation was to achieve sufficient cell engraftment and survival. With respect to treating liver-based inherited metabolic deficiencies and liver failures, liver transplantation is well established as an effective final option.[27] However, the progressive demand for transplantable livers far outweighs the donated organ supply.[28] Because this donor shortage issue will likely never be resolved, investigators have been prompted to search for alternate treatment options, including the creation of new cell-based therapies using hepatocytes. Researchers have transplanted hepatocytes into several different extrahepatic sites, including the intraperitoneal cavity, the pancreas, the mesenteric leaves, the lung parenchyma, under the kidney capsule, and in the subcutaneous space. It has been shown that providing ECMs to heterotopically transplanted hepatocytes affords significantly greater hepatocyte survival.[29] In the liver, hepatic cells are surrounded by the ECM that is important for functional and structural maintenance through cell–cell and cell–ECM interactions.[30,31] The intact liver is enwrapped within a capsule that is mainly composed of collagen fibrils and fibroblasts. Taking account of this liver architecture, we have generated a liver organoid tissue with a collagen fibril matrix, using a bioreactor to generate an artificial tissue *in vitro*. The histological structure of this construct is close to that of the liver itself. The liver organoid tissue has been experimentally investigated by transplantation into extrahepatic sites. To easily visualize the transplanted hepatocytes, Hep G2^{Red} cells, constitutively expressing DsRed were used during the preparation of the liver organoid tissue for transplantation. The transplanted liver organoid tissue revealed the formation of microvascular networks throughout the tissue constructs, indicating that integration with the host animal had occurred. This liver organoid tissue will be useful for applications related to transplantation.

The transplantation of the liver organoid tissue to the mesenteric vessels inside the intraperitoneal cavity has several advantages: it permits the transplantation of a cell number that is equivalent to an intact liver, the transplantation of genetically altered cells, and the engraftment of transplanted cells. The present study demonstrated that providing a condensed collagen fibril matrix in the transplantation contributed to increased hepatic cell engraftment, and to the stable survival of hepatic cells. These hepatic aggregates had a collagen density approaching endogenous tissue levels, and are mechanically suitable for *in vivo* implantation. Based on the lack of sufficient vascular support for the transplanted hepatocytes (not shown), we expected that establishing a local vascular network at the transplantation site would allow for nutrient and gas exchange with the grafts and that this would reduce graft loss.

In conclusion, by considering the 3D interactions between hepatocytes and the ECM, we made progress toward developing a liver model. The advantage of our system is that it consists of an artificial hepatic construct, which is structurally similar to the anatomical structures that occur naturally in the liver. The organoid tissue can be generated in a bioreactor within 24 h, and could serve as a model tissue to study the intrahepatic functions of various cells, cytokines, and ECMs. By mimicking the structure of the natural liver, our system effectively maintains multiple functions of liver tissue.

Acknowledgments

This study was supported by a Grant-in-Aid for Scientific Research (B) (No. 21300178 and 22300167) from the Japan Society for the Promotion of Science (JSPS); and a Grant-in-Aid for Scientific Research on Innovative Areas (No.

23119003) from the Ministry of Education, Culture, Sports, Science and Technology (MEXT) of Japan. Miho Tamai was supported by a Research Fellowship from JSPS.

Disclosure Statement

The authors who have taken part in this study declared that they do not have anything to disclose regarding funding or conflict of interests with respect to this article.

References

1. Di Lullo, G.A., Sweeney, S.M., Korkko, J., Ala-Kokko, L., and San Antonio, J.D. Mapping the ligand-binding sites and disease-associated mutations on the most abundant protein in the human, type I collagen. J Biol Chem **277,** 4223, 2002.
2. Wood, R.L., Kelly, D.E., Bailey, F.R., and Copenhaver, W.M. Bailey's Textbook of Histology. Williams & Wilkins, Baltimore, MD, 1978.
3. Marion, T.L., Leslie, E.M., and Brouwer, K.L. Use of sandwich-cultured hepatocytes to evaluate impaired bile acid transport as a mechanism of drug-induced hepatotoxicity. Mol Pharmacol **4,** 911, 2007.
4. Berthiaume, F., Moghe, P.V., Toner, M., and Yarmush, M.L. Effect of extracellular matrix topology on cell structure, function, and physiological responsiveness: hepatocytes cultured in a sandwich configuration. FASEB J **10,** 1471, 1996.
5. Dunn, J.C., Yarmush, M.L., Koebe, H.G., and Tompkins, R.G. Hepatocyte function and extracellular matrix geometry: long-term culture in a sandwich configuration. FASEB J **3,** 174, 1989.
6. Michalopoulos, G., Sattler, C.A., Sattler, G.L., and Pitot, H.C. Cytochrome P-450 induction by phenobarbital and 3-methylcholanthrene in primary cultures of hepatocytes. Science **193,** 907, 1976.
7. Toyoda, Y., Tamai, M., Kashikura, K., Kobayashi, S., Fujiyama, Y., Soga, T., and Tagawa, Y. Acetaminophen-induced hepatotoxicity in a liver tissue model consisting of primary hepatocytes assembling around an endothelial cell network. Drug Metab Dispos **40,** 169, 2012.
8. Ben-Ze'ev, A., Robinson, G.S., Bucher, N.L., and Farmer, S.R. Cell-cell and cell-matrix interactions differentially regulate the expression of hepatic and cytoskeletal genes in primary cultures of rat hepatocytes. Proc Natl Acad Sci U S A **85,** 2161, 1988.
9. Trautwein, C., Davies, M., Elias, E., Strain, A., and Manns, M.P. Extracellular matrix proteins modulate cytochrome P450 2D6 expression in human hepatocytes. J Hepatol **22,** 50, 1995.
10. Skardal, A., Smith, L., Bharadwaj, S., Atala, A., Soker, S., and Zhang, Y. Tissue specific synthetic ECM hydrogels for 3-D *in vitro* maintenance of hepatocyte function. Biomaterials **33,** 4565, 2012.
11. Kim, Y., and Rajagopalan, P. 3D hepatic cultures simultaneously maintain primary hepatocyte and liver sinusoidal endothelial cell phenotypes. PLoS One **5,** 15456, 2010.
12. Kim, M., Lee, J.Y., Jones, C.N., Revzin, A., and Tae, G. Heparin-based hydrogel as a matrix for encapsulation and cultivation of primary hepatocytes. Biomaterials **31,** 3596, 2010.
13. Ananthanarayanan, A., Narmada, B.C., Mo, X., McMillian, M., and Yu, H. Purpose-driven biomaterials research in liver-tissue engineering. Trends Biotechnol **29,** 110, 2011.
14. Kim, Y., Lasher, C.D., Milford, L.M., Murali, T.M., and Rajagopalan, P. A comparative study of genome-wide transcriptional profiles of primary hepatocytes in collagen sandwich and monolayer cultures. Tissue Eng Part C Methods **16,** 1449, 2010.
15. Mathijs, K., Kienhuis, A.S., Brauers, K.J., Jennen, D.G., Lahoz, A., Kleinjans, J.C., and van Delft, J.H. Assessing the metabolic competence of sandwich-cultured mouse primary hepatocytes. Drug Metab Dispos **37,** 1305, 2009.
16. Giri, S., Acikgoz, A., Pathak, P., Gutschker, S., Kursten, A., Nieber, K., and Bader, A. Three dimensional cultures of rat liver cells using a natural self-assembling nanoscaffold in a clinically relevant bioreactor for bioartificial liver construction. J Cell Physiol **227,** 313, 2012.
17. Sudo, R., Mitaka, T., Ikeda, M., and Tanishita, K. Reconstruction of 3D stacked-up structures by rat small hepatocytes on microporous membranes. FASEB J **19,** 1695, 2005.
18. Martinez-Hernandez, A., and Amenta, P.S. The hepatic extracellular matrix. I. Components and distribution in normal liver. Virchows Arch A Pathol Anat Histopathol **423,** 1, 1993.
19. Iwashiro, H., Hosoya, S., Hirai, K., Mima, T., Ohashi, S., Aihara, T., Ito, S., Ohara, S., and Adachi, E. Characterization of dense artificial connective tissues generated in a newly designed bioreactor. Connect Tissue Res **52,** 340, 2011.
20. Seglen, P.O. Preparation of isolated rat liver cells. Methods Cell Biol **13,** 29, 1976.
21. Ryu, J.Y., Siswanto, A., Harimoto, K., and Tagawa, Y.I. Chimeric analysis of EGFP and DsRed2 transgenic mice demonstrates polyclonal maintenance of pancreatic acini. Transgenic Res, 2012. DOI:10.1007/s11248-012-9661-8.
22. Tsutsui, M., Ogawa, S., Inada, Y., Tomioka, E., Kamiyoshi, A., Tanaka, S., Kishida, T., Nishiyama, M., Murakami, M., Kuroda, J., Hashikura, Y., Miyagawa, S., Satoh, F., Shibata, N., and Tagawa, Y. Characterization of cytochrome P450 expression in murine embryonic stem cell-derived hepatic tissue system. Drug Metab Dispos **34,** 696, 2006.
23. Griffith, L.G., and Naughton, G. Tissue engineering—current challenges and expanding opportunities. Science **295,** 1009, 2002.
24. Shin, H., Jo, S., and Mikos, A.G. Biomimetic materials for tissue engineering. Biomaterials **24,** 4353, 2003.
25. Gerlach, J.C., Mutig, K., Sauer, I.M., Schrade, P., Efimova, E., Mieder, T., Naumann, G., Grunwald, A., Pless, G., Mas, A., Bachmann, S., Neuhaus, P., and Zeilinger, K. Use of primary human liver cells originating from discarded grafts in a bioreactor for liver support therapy and the prospects of culturing adult liver stem cells in bioreactors: a morphologic study. Transplantation **76,** 781, 2003.
26. Hamilton, G.A., Jolley, S.L., Gilbert, D., Coon, D.J., Barros, S., and LeCluyse, E.L. Regulation of cell morphology and cytochrome P450 expression in human hepatocytes by extracellular matrix and cell-cell interactions. Cell Tissue Res **306,** 85, 2001.
27. Crespo, G., Marino, Z., Navasa, M., and Forns, X. Viral hepatitis in liver transplantation. Gastroenterology **142,** 1373, 2012.
28. Ogawa, S., and Miyagawa, S. Potentials of regenerative medicine for liver disease. Surg Today **39,** 1019, 2009.
29. Ohashi, K., Yokoyama, T., Yamato, M., Kuge, H., Kanehiro, H., Tsutsumi, M., Amanuma, T., Iwata, H., Yang, J., Okano, T., and Nakajima, Y. Engineering functional two- and three-

dimensional liver systems *in vivo* using hepatic tissue sheets. Nat Med **13**, 880, 2007.
30. Bhatia, S.N., Balis, U.J., Yarmush, M.L., and Toner, M. Effect of cell-cell interactions in preservation of cellular phenotype: cocultivation of hepatocytes and nonparenchymal cells. FASEB J **13**, 1883, 1999.
31. Liu, L., Yannam, G.R., Nishikawa, T., Yamamoto, T., Basma, H., Ito, R., Nagaya, M., Dutta-Moscato, J., Stolz, D.B., Duan, F., Kaestner, K.H., Vodovotz, Y., Soto-Gutierrez, A., and Fox, I.J. The microenvironment in hepatocyte regeneration and function in rats with advanced cirrhosis. Hepatology **55**, 1529, 2012.

Address correspondence to:
Yoh-ichi Tagawa, DSc
Department of Biomolecular Engineering
Graduate School of Bioscience and Biotechnology
Tokyo Institute of Technology
4259 B-51 Nagatsuta-cho Midori-ku, Yokohama
Kanagawa 226-8501
Japan

E-mail: ytagawa@bio.titech.ac.jp

Received: November 29, 2012
Accepted: June 19, 2013
Online Publication Date: August 22, 2013

JVI
Journals.ASM.org

Japanese Encephalitis Virus Core Protein Inhibits Stress Granule Formation through an Interaction with Caprin-1 and Facilitates Viral Propagation

Hiroshi Katoh,[a] Toru Okamoto,[a] Takasuke Fukuhara,[a] Hiroto Kambara,[a] Eiji Morita,[b] Yoshio Mori,[d] Wataru Kamitani,[c] Yoshiharu Matsuura[a]

Department of Molecular Virology,[a] International Research Center for Infectious Diseases,[b] and Global COE Program,[c] Research Institute for Microbial Diseases, Osaka University, Osaka, Japan; Department of Virology III, National Institute of Infectious Diseases, Tokyo, Japan[d]

Stress granules (SGs) are cytoplasmic foci composed of stalled translation preinitiation complexes induced by environmental stress stimuli, including viral infection. Since viral propagation completely depends on the host translational machinery, many viruses have evolved to circumvent the induction of SGs or co-opt SG components. In this study, we found that expression of Japanese encephalitis virus (JEV) core protein inhibits SG formation. Caprin-1 was identified as a binding partner of the core protein by an affinity capture mass spectrometry analysis. Alanine scanning mutagenesis revealed that Lys^{97} and Arg^{98} in the α-helix of the JEV core protein play a crucial role in the interaction with Caprin-1. In cells infected with a mutant JEV in which Lys^{97} and Arg^{98} were replaced with alanines in the core protein, the inhibition of SG formation was abrogated, and viral propagation was impaired. Furthermore, the mutant JEV exhibited attenuated virulence in mice. These results suggest that the JEV core protein circumvents translational shutoff by inhibiting SG formation through an interaction with Caprin-1 and facilitates viral propagation *in vitro* and *in vivo*.

In eukaryotic cells, environmental stresses such as heat shock, oxidative stress, UV irradiation, and viral infection trigger a sudden translational arrest, leading to stress granule (SG) formation (1). SGs are cytoplasmic foci composed of stalled translation preinitiation complexes and are postulated to play a critical role in regulating mRNA metabolism during stress via so-called "mRNA triage" (2). The initiation of SG formation results from phosphorylation of eukaryotic translation initiation factor 2α (eIF2α) at Ser^{51} by various kinases, including protein kinase R (PKR), PKR-like endoplasmic reticulum kinase (PERK), general control nonrepressed 2 (GCN2), and heme-regulated translation inhibitor (HRI), which are commonly activated by double-stranded RNA (dsRNA), endoplasmic reticulum (ER) stress, nutrient starvation, and oxidative stress, respectively. Phosphorylation of eIF2α reduces the amount of eIF2-GTP-tRNA complex and inhibits translation initiation, leading to runoff of elongating ribosomes from mRNA transcripts and the accumulation of stalled translation preinitiation complexes. Thus, SGs are defined by the presence of components of translation initiation machinery, including 40S ribosome subunits, poly(A)-binding protein (PABP), eIF2, eIF3, eIF4A, eIF4E, eIF4G, and eIF5. Then, primary aggregation occurs through several RNA-binding proteins (RBPs), including T-cell intracellular antigen-1 (TIA-1), TIA-1-related protein 1 (TIAR), and Ras-Gap-SH3 domain-binding protein (G3BP). These RBPs are independently self-oligomerized with the stalled initiation factors and with other RBPs, such as USP10, hnRNP Q, cytoplasmic activation/proliferation-associated protein-1 (Caprin-1), and Staufen and with nucleated mRNA-protein complex (mRNP) aggregations (3, 4). SG assembly begins with the simultaneous formation of numerous small mRNP granules which then progressively fuse into larger and fewer structures, a process known as secondary aggregation (5). The aggregation of TIA-1 or TIAR is regulated by molecular chaperones, such as heat shock protein 70 (Hsp70) (3), whereas that of G3BP is controlled by its phosphorylation at Ser^{149} (4). SG formation and disassembly in response to cellular stresses are strictly regulated by multiple factors.

Viral infection can certainly be viewed as a stressor for cells, and SGs have been reported in some virus-infected cells. Since the propagation of viruses is completely reliant on the host translational machinery, stress-induced translational arrest plays an important role in host antiviral defense. To antagonize this host defense, most viruses have evolved to circumvent SG formation during infection. For example, poliovirus (PV) proteinase 3C cleaves G3BP, leading to effective SG dispersion and virus propagation (6). Influenza A virus nonstructural protein 1 (NS1) has been shown to inactivate PKR and prevent SG formation (7). In the case of human immunodeficiency virus 1 (HIV-1) infection, Staufen1 is recruited in ribonucleoproteins for encapsidation through interaction with the Gag protein to prevent SG formation (8). In contrast, some viruses employ alternative mechanisms of translation initiation and promote SG formation to limit cap-dependent translation of host mRNA (9, 10). In addition, vaccinia virus induces cytoplasmic "factories" in which viral translation, replication, and assembly take place. These factories include G3BP and Caprin-1 to promote transcription of viral mRNA (11).

Japanese encephalitis virus (JEV) belongs to the genus *Flavivirus* within the family *Flaviviridae*, which includes other mosquito-borne human pathogens, such as dengue virus (DENV), West Nile virus (WNV), and yellow fever virus, that frequently cause significant morbidity and mortality in mammals and birds (12). JEV has

Received 15 August 2012 Accepted 15 October 2012
Published ahead of print 24 October 2012
Address correspondence to Yoshiharu Matsuura, matsuura@biken.osaka-u.ac.jp.

doi:10.1128/JVI.02186-12